Theory of high-T_c superconductors within an Anderson lattice model

D. M. Newns
IBM Research Division, Thomas J. Watson Research Center, Yorktown Heights, New York 10598

Mark Rasolt
Solid State Division, Oak Ridge National Laboratory, Oak Ridge, Tennessee 37831

P. C. Pattnaik
IBM Research Division, Thomas J. Watson Research Center, Yorktown Heights, New York 10598
(Received 7 January 1988)

An Anderson lattice model for high-T_c superconductors, in particular $La_{2-x}Sr_xCuO_4$, is set up and explicitly transformed into a slave-boson representation. The model is solved using a formal $1/N$ expansion technique, where N is the degeneracy of the d^9 state, working to leading-N approximation in the normal state and $O(1/N)$ in the superconducting state. Normal-state properties such as susceptibility, density of states, and the location of added holes are calculated and compared with experiment. The model is an s-wave superconductor in the present approximation for realistic parameters. The gap-to-T_c ratio, specific-heat jump, and $H_c(0)$ take their Bardeen-Cooper-Schrieffer values. The variation of T_c with doping is successfully explained. A calculation of the critical region, taking into account strong tetragonal anisotropy, finds its width of order 1 K, in agreement with experiment.

I. INTRODUCTION

The family of high-T_c superconductors, such as $La_{2-x}Sr_xCuO_4$ (2:1:4), now including the 1:2:3, 2:2:1:2, and 2:2:2:3 compounds, pose two fundamental, linked, theoretical questions. First, how to describe the normal phase, and second, the nature of the superconductivity, questions which can only be posed in the framework of the overall experimental picture.

The common structural feature of these materials is the presence of the well-known CuO_2 planes. The role of the rest of the material seems principally to be to control the doping of the planes. As a result of doping, the planes contain a concentration x_h of holes in the range 0–0.3 per $Cu^{2+}O_2^{2-}$ unit. Band structure[1–3] shows that both 2:1:4 and 1:2:3 materials have copper d bands strongly hybridized with oxygen bands, and predicts metallic character, with the Fermi level lying in bands consisting mostly of O p_x, O p_y, and $d_{x^2-y^2}$ orbitals. The copper valence state lies between d^9 and d^{10} despite the nominal valence between d^8 and d^9.

At zero doping the better investigated materials (2:1:4 and 1:2:3) are antiferromagnetic insulators,[4] in contrast to the metallic band-structure picture. The doped materials, however, seem to show Fermi-liquid behavior. Evidence for this comes from the sharp Fermi edge in photoemission and inverse photoemission,[5] and from positron annihilation.[6] Consistent with Fermi-liquid properties is the Drude behavior of the dielectric function.[7] Thermodynamic evidence from the specific-heat jump[8] and the Pauli susceptibility[9] also supports the Fermi-liquid nature of the doped phase. Doping, however, results in the holes going into the oxygen $2p$ orbitals rather than into the Cu $3d$ orbitals.[10]

The chief properties of the superconducting phase are that the pairing is singlet,[11] and probably s wave[12,13] though the evidence on the latter point is confusing at the moment. The gap-to-T_c ratio is about twice the BCS value,[7,14] while the width of the critical region is observed to be about 1 K.[15] The isotope index[16] falls off from a BCS value of 0.5 in $La_{2-x}Ca_xCuO_4$ ($T_c=20$ K) to 0.15 in $La_{1.85}Sr_{0.15}CuO_4$ ($T_c=39$ K) to 0.01 in $YBa_2Cu_3O_7$ ($T_c=92$ K). Presumably, this indicates that a nonphonon pairing mechanism is increasingly important as T_c increases. The materials are strongly type II.[17]

In the Fermi-liquid phase the materials show signs of strong electron correlation, which first of all can be inferred from the presence of the phase boundary with the antiferromagnetic insulator. Additional evidence comes from the enhancement of the Pauli susceptibility,[9] suggesting an m^*/m between 4 and 8 (according to definition), approaching the values in heavy-fermion materials, and secondly from the Hall effect.[18–20] The Hall number is hole type in sign and scales roughly with x_h. This has recently been explained in the Fermi-liquid picture with large Landau parameters,[21] but it cannot be explained in a noninteracting electron-gas picture.

The correlation effects probably originate in a Hubbard U within the Cu d orbitals. This is supported, e.g., by the observation of a two-hole satellite in photoemission spectra.[22] U is usually considered to be 6–7 eV.[22] The existence of a U will lead to important effects in the normal state such as the enhancement of χ and γ.[23] However, in such U-enhanced systems the quasiparticles have a reduced coupling to charge excitations. Hence superconductivity from coupling to charge-fluctuation modes such as phonons, plasmons, and excitons is unlikely.

The most likely origin for superconductivity in large-U systems is then an indirect one via U itself. One approach to this is that of Anderson,[24] who points out that a description of a half-filled Hubbard band (derived from Cu d orbitals) in terms of a configuration of pair bonds is

a form of real-space pairing. This approach has been developed by a canonical transformation into an infinite-U model with a nearest-neighbor antiferromagnetic Heisenberg interaction, and solved within mean field[24–26] or using the coherent potential approximation (CPA).[27] Another approach, due to one of us,[28] developed earlier for the theory of heavy-fermion superconductivity,[29] starts from the Anderson lattice model, and retains the finite U explicitly. The model is solved within the framework of a normal $1/N$ expansion. We think that this approach has advantages in a system where the band structure clearly shows O-Cu hybridization to be playing a crucial role, as discussed in more detail in the conclusion. That the hybridization with the oxygen bands is indeed essential for superconductivity is seen in recent Monte Carlo simulations,[30,31] limited though these are to temperatures of order 1000 K or higher. The simulations suggest that the Hubbard model on a square lattice is not superconducting, while the model put forward independently by Emery[32] and Hirsch[31] is superconducting. This model is a simplified version of an Anderson lattice model, in which the Cu $d_{x^2-y^2}$ orbitals hybridize with the nearest-neighbor oxygen atoms but the latter have no other couplings. There is no intrinsic oxygen bandwidth.

A recent study of a one-dimensional model including oxygen bands showed that the model can be a triplet superconductor,[33] but it is not as yet a rotationally invariant model so the conclusions so far need to be accepted with caution. A different philosophy is to invoke antiferromagnetic magnons as the mediating interaction, but then s-wave pairing is difficult to achieve.[34,35]

To arrive at reliable conclusions, arbitrary approximations need to be developed into systematic procedures, of which Monte Carlo simulations at sufficiently low-temperature, low-dimensional models and $1/N$ expansions are examples. In this paper then, we shall work with the $1/N$ expansion technique, developing the theory as clearly as possible. In this paper we give results only to leading order in $1/N$. Higher-order corrections will be the subject of a future paper.

II. ANDERSON LATTICE MODEL IN SLAVE-BOSON REPRESENTATION

In oxide superconductors there are large hopping matrix elements connecting the Cu atoms to neighboring oxygen atoms, and also direct and indirect matrix elements connecting the oxygen atoms to each other, the latter being sometimes neglected. However, these neglected matrix elements lead to an oxygen bandwidth of around 4 eV. When renormalization of the copper-oxygen hopping, due to the Hubbard U on the Cu atoms, and also shifts breaking the approximate degeneracy of the Cu and oxygen orbitals, are taken into account, neglect of all but the Cu-oxygen hopping matrix element seems to be an inaccurate approximation to the electronic structure.

In this paper we shall concentrate on the $La_{2-x}Sr_xCuO_4$ materials, which seem to be the simplest class, although we believe the other groups are very similar. The model we use is then the typical Anderson lattice model used in heavy-fermion systems, which can describe all electronic structure effects. The basis set involves in its most general form a set of oxygen bands denoted by band index α, with wave vector $\mathbf{k}$ in the first Brillouin zone (BZ), giving states $|\mathbf{k}\alpha\rangle$ of energy $\varepsilon_{\mathbf{k}\alpha}$. Copper d orbitals $|id\gamma\rangle$ on lattice site i are defined where single-particle energy in the absence of a Hubbard U on the Cu site would be $E_{1\gamma}$. Matrix elements $V_{\mathbf{k}}=\langle 0d\gamma|V|\mathbf{k}\alpha\rangle$ define the hopping amplitude from an atomic d state γ at the origin to an itinerant O state in the band α. The present paper is concerned chiefly with analytic results, and therefore we treat an analytically solvable model.

Specializing to the frequently considered model of an isolated layer of Cu and oxygen atoms in the La-Sr-Cu-O structure, only the d orbital $d_{x^2-y^2}$ is usually considered to be partially occupied, and we alone include it in the basis set as $|id\rangle$. Again, oxygen holes are assumed to be confined to the p_x,p_y orbitals directly coupled to the $d_{x^2-y^2}$ orbital. Including these orbitals alone gives two oxygen bands. We further simplify the model by making an artificial separation of the bands into a nonbonding band, which does not hybridize with the copper $d_{x^2-y^2}$, and a hybridizing band $|\mathbf{k}\rangle$. Finally, we choose to work with hole rather than electron states. In terms then of the states $|id\rangle$ and $|\mathbf{k}\rangle$, the Anderson lattice model is

$$\mathcal{H}=\sum_{\mathbf{k}\sigma}\varepsilon_{\mathbf{k}}c^{\dagger}_{\mathbf{k}\sigma}c_{\mathbf{k}\sigma}+E_1\sum_{i\sigma}D^{\dagger}_{i\sigma}D_{i\sigma}+\sum_{\mathbf{k}i\sigma}(V_{\mathbf{k}}D^{\dagger}_{i\sigma}c_{\mathbf{k}\sigma}e^{i\mathbf{k}\cdot\mathbf{r}_i}+\text{H.c.})+U\sum_i N_{di\sigma}N_{di-\sigma}. \quad (2.1)$$

Here the $c_{\mathbf{k}\sigma}$ are fermion operators for holes of spin σ in the O band of Bloch wave vector $\mathbf{k}$ in the first BZ, and the $D_{i\sigma}$ are fermion operators for spin σ holes in the $d_{x^2-y^2}$ orbital on lattice site i, located at $\mathbf{r}_i$. Also $N_{id\sigma}=D^{\dagger}_{i\sigma}D_{i\sigma}$.

Assuming $U=0$, the model (2.1) can be used to generate an oxygen density of states (DOS) with the E_1 level at the center of the O band, and compared with Matheiss's calculation. Even using a square model of the DOS in the oxygen band, a fair picture of the DOS in the Mattheiss calculation results (see below).

The four-fermion term involving the Hubbard or Anderson U is inconvenient when U is large. In this paper it is transformed by defining explicitly operators to represent the d^8, d^9, and d^{10} configurations of a Cu atom. The required basis set or "slave-boson" representation[29,36] may be most conveniently introduced via an ansatz for the $D_{i\sigma}$ and $D_{i\sigma}$ operators previously set up for the Hubbard model[37]

$$D_{i\sigma}=b^{\dagger}_i d_{i\sigma}+\text{sgn}(\sigma)a d^{\dagger}_{i-\sigma},\qquad D^{\dagger}_{i\sigma}=b_i d^{\dagger}_{i\sigma}+\text{sgn}(\sigma)a^{\dagger}d_{i-\sigma}. \quad (2.2)$$

In (2.2), b_i and a_i are bosons representing the d^{10} and d^8 states (both singlets) of the Cu ion, respectively. Of course d^8 is a singlet only because of the strong tetragonal crystal field (or "ligand field") in oxide superconductors. The d^9 state is represented by a fermion (sometimes termed spinon[25]) $d_{i\sigma}$ with spin σ.

Evidently, we require that the original fermions $D_{i\sigma}$ anticommute. Substituting (2.2) into the anticommutator, we obtain

$$\{D_{i\sigma},D^{\dagger}_{i\sigma}\}=Q_i, \quad (2.3)$$

where

$$Q_i = a_i^\dagger a_i + b_i^\dagger b_i + \sum_\sigma d_{i\sigma}^\dagger d_{i\sigma} = 1 . \tag{2.4}$$

The important relationship (2.4) can be thought of as a normalization constraint on the overcomplete basis of a, b, and d_σ. It restricts physical operators to the subspace of physically allowed states where three of these four operators have zero, and the fourth unit, eigenvalue. The derivations in this section make use of this restriction.

The number operator for spin σ on a d site is from (2.2)

$$N_{id\sigma} = D_{i\sigma}^\dagger D_{i\sigma} = a_i^\dagger a_i + d_{i\sigma}^\dagger d_{i\sigma} , \tag{2.5}$$

and the total d-number operator is

$$\sum_\sigma N_{id\sigma} = 2a_i^\dagger a_i + \sum_\sigma d_{i\sigma}^\dagger d_{i\sigma} = a_i^\dagger a_i - b_i^\dagger b_i + 1 . \tag{2.6}$$

Now we may substitute (2.2) and (2.5) into (2.1) to obtain the Hamiltonian in slave-boson representation,

$$\mathcal{H} = \sum_{\mathbf{k}\sigma} \varepsilon_{\mathbf{k}} c_{\mathbf{k}\sigma}^\dagger c_{\mathbf{k}\sigma} + E_2 \sum_i a_i^\dagger a_i + E_1 \sum_{i\sigma} d_{i\sigma}^\dagger d_{i\sigma} + \sum_{\mathbf{k}i\sigma} [V_{\mathbf{k}} (b_i d_{i\sigma}^\dagger + a_i^\dagger d_{i-\sigma} \mathrm{sgn}\sigma) c_{\mathbf{k}\sigma} e^{i\mathbf{k}\cdot\mathbf{r}_i} + \mathrm{H.c.}] . \tag{2.7}$$

In (2.7), E_2 is the energy of the two-hole (d^8) Cu state, $E_2 \equiv 2E_1 + U$. The energy of the d^{10} state is defined to be zero. The $V_{\mathbf{k}}$ terms are more complicated than in (2.1). They represent processes whereby in the first term, a d^9 of spin σ may be created by annihilating a d^{10} and a conduction hole of the same spin, or (second term) by annihilating a d^8 state and creating a conduction hole conjugate of opposite spin.

The global number operator is constructed from (2.6) as

$$\hat{N} = 2\sum_i a_i^\dagger a_i + \sum_{i\sigma} d_{i\sigma}^\dagger d_{i\sigma} + \sum_{\mathbf{k}\sigma} c_{\mathbf{k}\sigma}^\dagger c_{\mathbf{k}\sigma} \tag{2.8}$$

and commutes with $\mathcal{H}$. In grand-canonical ensemble we work with

$$\mathcal{H}' = \mathcal{H} - \mu\hat{N} , \tag{2.9}$$

where μ is chemical potential.

Now (2.7) is an insoluble model (albeit not usually written thus). Our approach is to generate a suite of models characterized by even index N, of which our model with $N=2$ is the lowest member, and which are soluble in the large-N limit. Then by expansion in $1/N$ we hope to extrapolate to the real, $N=2$, model.

For infinite U the conventional procedure is to define d^{10} as a singlet and d^9 as an N-let, where $N=2n$ and n is an orbital degeneracy. As regards d^8, in our picture of superconductivity, the key role of the d^8 state is to provide a relatively high-lying scattering resonance which near T_c renormalizes into the Azlamazov-Larkin two-particle propagator, and thus has the symmetry of the order parameter. Hence we are principally interested in the component of d^8 retaining ^1S symmetry at each n, whose wave function is

$$|\Psi\rangle = n^{-1/2} \sum_{\mu=1}^{n} c_{\mu\uparrow}^\dagger c_{\mu\downarrow}^\dagger |\mathrm{vac}\rangle , \tag{2.10}$$

where μ is the orbital channel. We shall consider other components of the hypothetical orbitally degenerate d^8 state to be irrelevant, and thus define (2.10) as the a boson. The matrix element between (2.10) and the d^9 state is then $V_{\mathbf{k}}' = n^{-1/2} V_{\mathbf{k}}$. Defining $m = \{n,\sigma\}$, the Nth of the suite has the Hamiltonian

$$\mathcal{H} = \sum_{\mathbf{k}m} \varepsilon_{\mathbf{k}} c_{\mathbf{k}m}^\dagger c_{\mathbf{k}m} + E_2 \sum_i a_i^\dagger a_i + E_1 \sum_{i\sigma} d_{im}^\dagger d_{im} + \sum_{\mathbf{k}im} V_{\mathbf{k}} b_i d_{im}^\dagger c_{\mathbf{k}m} e^{i\mathbf{k}\cdot\mathbf{r}_i} + \mathrm{H.c.} + \sum_{\mathbf{k}im} V_{\mathbf{k}}' a_i^\dagger d_{i-m} c_{\mathbf{k}m} e^{i\mathbf{k}\cdot\mathbf{r}_i} + \mathrm{H.c.} , \tag{2.11}$$

$$Q_i = a_i^\dagger a_i + b_i^\dagger b_i + \sum_m d_{im}^\dagger d_{im} = \mathbf{q}N , \tag{2.12}$$

$$\hat{N} = 2\sum_i a_i^\dagger a_i + \sum_{im} d_{im}^\dagger d_{im} + \sum_{\mathbf{k}m} c_{\mathbf{k}m}^\dagger c_{\mathbf{k}m} , \tag{2.13}$$

$$N_{di} = 2a_i^\dagger a_i + \sum_m d_{im}^\dagger d_{im} . \tag{2.14}$$

The commutation relations $[Q_i,\mathcal{H}]=0$, $[\hat{N},\mathcal{H}]=0$ are preserved. In (2.12), $\mathbf{q}$ is defined to be O(1) and then set equal to $1/N$ at the end of the calculation. We do not wish to delude the reader that (2.11)–(2.13) for $N>2$ have physical meaning, but prefer to regard them as merely analytic continuations of the physical model.

The operator Q_i, commuting as it does with $\mathcal{H}$, constitutes a local symmetry of the model. Consider Q_i as the generator of a transformation, $U = \exp(iQ_i\phi)$. Then

$$U^\dagger A_i U = A_i e^{i\phi} , \tag{2.15}$$

where $A_i = a_i$, b_i, or $d_{i\sigma}$. We see that Q_i in fact generates a local gauge symmetry. This symmetry is a consequence of our writing $\mathcal{H}$ in terms of an overcomplete basis. Physical quantities must be invariant under (2.15), for example $N_{id\sigma}$.

The conventional choice of order parameter for a singlet superconductor would be

$$\Phi = \sum_{\mathbf{k}\sigma} \langle c_{\mathbf{k}\sigma} c_{-\mathbf{k}-\sigma} \rangle f(\mathbf{k}) \mathrm{sgn}\sigma , \tag{2.16}$$

where $f(\mathbf{k})$ (even in $\mathbf{k}$) is a form factor large only for states near the Fermi level. If we worked in the d subspace, a similar choice would be

$$\Phi' = \sum_{ij\sigma} \langle D_{i\sigma} D_{j-\sigma} \rangle g(\mathbf{r}_i - \mathbf{r}_j) \mathrm{sgn}\sigma , \tag{2.17}$$

where g is a form factor in real space analogous to the Fourier transform of f. Writing (2.17) in terms of (2.2), we have

$$\Phi' = \sum_{ij\sigma} \mathrm{sgn}(\sigma) g(\mathbf{r}_i - \mathbf{r}_j) (\langle b_i^\dagger b_j^\dagger d_{i\sigma} d_{j-\sigma} \rangle + \langle a_i a_j d_{i-\sigma}^\dagger d_{j\sigma}^\dagger \rangle + \mathrm{sgn}\sigma \langle a_i b_j^\dagger d_{i-\sigma}^\dagger d_{j-\sigma} \rangle - \mathrm{sgn}\sigma \langle a_j b_i^\dagger d_{i\sigma} d_{j\sigma}^\dagger \rangle) \tag{2.18}$$

or

$$\Phi' = \sum_{i\neq j\sigma} g(\mathbf{r}_i - \mathbf{r}_j) (\langle b_i^\dagger b_j^\dagger d_{i\sigma} d_{j-\sigma} \rangle \mathrm{sgn}\sigma + \langle a_i a_j d_{i-\sigma}^\dagger d_{j\sigma}^\dagger \mathrm{sgn}\sigma + 2\langle a_i b_j^\dagger d_{i\sigma}^\dagger d_{j\sigma} \rangle) - 2g(0) \sum_i \langle b_i^\dagger a_i \rangle . \tag{2.19}$$

The simplest component of the order parameter in the d subspace is the one involving $\langle a_i b_i^\dagger \rangle$. It is seen to be local gauge invariant. Moreover, it rotates under a gauge transformation whose generator is the local number operator (2.6), as it should. Presumably, when this order parameter becomes nonzero, so does (2.16) and (2.17). However, other components in (2.19) could also cause nonzero Φ'. The order parameter $\langle a_i b_i^\dagger \rangle$ does not imply Bose condensation, but rather b boson to a antiboson pairing. However, since the a-boson propagator diverges at T_c, a superficial resemblance to Bose condensation indeed appears.

Finally, it is interesting to see how the appropriate superconducting order parameter emerges from the consideration of current-current response functions of the paramagnetic current $j_\mu(\mathbf{x})$. Such current-current response functions $\mathbf{k}_{\mu\nu}(\mathbf{x}_1 - \mathbf{x}_2)$ are given by

$$k_{\mu\nu}(\mathbf{x}_1 - \mathbf{x}_2) = \langle j_\mu(\mathbf{x}_1) j_\nu(x_2) \rangle , \tag{2.20}$$

where

$$j_\mu(\mathbf{x}) = \psi^\dagger(\mathbf{x}) \frac{\partial \psi(\mathbf{x})}{\partial x_\mu} - \psi(\mathbf{x}) \frac{\partial \psi^\dagger(\mathbf{x})}{\partial x_\mu} , \tag{2.21}$$

where $\psi(\mathbf{x})$ is the usual field operator for the c and d fermions. We draw in Fig. 1(a) a typical low-order Feynman graph of $k_{\mu\nu}$ corresponding to Eq (2.11) in the $N \rightarrow \infty$ limit (see the next section for a detailed discussion of the $N \rightarrow \infty$ mean-field limit). Now terms that remain invariant under the local gauge transformations of Eq. (2.15) are the crosses in the collapsed graphs of Fig. 1(b). Since the dashed propagator between $\mathbf{r}_i$ and $\mathbf{r}_j$ in Fig. 1(a) is given by $\langle d_{i\sigma}^\dagger d_{j\sigma} \rangle$, it is not difficult to see that the last two terms in Eq. (2.19) are retrieved. Furthermore, such current-current response functions, in terms of the crosses in Fig. 1(b), are identical to standard superconductivity.

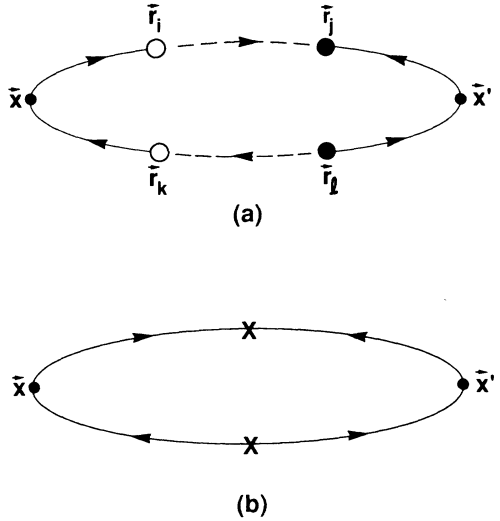

FIG. 1. (a) Low-order graphs for the current-current response functions. Open circles are V times the boson expectation value $\langle b_i \rangle$ and solid circles are V times the boson expectation value $\langle a_i \rangle$. Solid arrowed lines are the conduction free-electron propagators and dashed-arrowed lines are the localized-state free-electron propagators $\langle d_{i\sigma}^\dagger d_{i\sigma} \rangle$. (b) The same as (a) with $x \equiv V^2 \langle b_i \rangle d_{i\sigma}^\dagger d_{j\sigma} \langle a_j \rangle$.

III. LEADING-N SOLUTION IN NORMAL PHASE

In the parameter range in which we shall be working, the fraction of d^8 in the system, i.e., a^2, is very small, due to the relatively high energy E_2 of the d^8 state. Therefore, we shall assume that in the normal phase the a boson can be neglected [although, as can be seen from (2.19) it plays an essential role in the superconducting phase]. This is equivalent to treating the normal phase as a $U = \infty$ model. The treatment of the $U = \infty$ limit of (2.7) is well established.[38-40] First of all, at low temperatures ($T \ll T_K$, where the characteristic energy scale $T_K \simeq 0.5$ eV is defined below), the constraint on Q may be replaced by its mean-field value,[38-40] handled by adding to $\mathcal{H} - \mu \hat{N}$ a Lagrange multiplier term giving

$$\mathcal{H}' = \mathcal{H} - \mu \hat{N} + \lambda \sum_i (Q_i - qN) . \tag{3.1}$$

This point has been discussed in the present gauge by Millis and Lee.[41] Customarily, we redefine λ in terms of the quasiparticle d-level energy

$$\varepsilon_d = E_1 + \lambda . \tag{3.2}$$

Then $\mathcal{H}'$ becomes

$$\begin{aligned} \mathcal{H}' = & \sum_m \varepsilon_{\mathbf{k}} c_{\mathbf{k}m}^\dagger c_{\mathbf{k}m} + \varepsilon_d \sum_{im} d_{im}^\dagger d_{im} \\ & + \sum_{\mathbf{k}mi} (V_{\mathbf{k}} b_i d_{im}^\dagger c_{\mathbf{k}m} e^{i\mathbf{k}\cdot\mathbf{r}_i} + \text{H.c.}) \\ & + \sum_i (\varepsilon_d - E_1)(b^\dagger b - qN) - \mu \hat{N} . \end{aligned} \tag{3.3}$$

In (3.3), ε_d (i.e., λ) is to be determined variationally.

Now we see that (3.3) is a Hamiltonian of reasonably conventional type which can be treated by standard Feynman graph expansion techniques. In Fig. 2 we illustrate

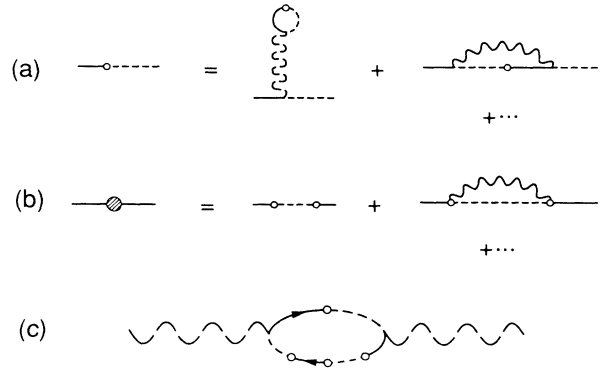

FIG. 2. (a) Graphs for the $\mathbf{k}d$ self-energy assuming the d^8 state (a boson) may be neglected. Broken wavy line and wavy line are bare b-boson propagator and b-boson propagator including self-energy of (b), respectively; otherwise notation same as in Fig. 1; (b) Graphs for $\mathbf{k}\mathbf{k}$ self-energy; (c) leading order in $1/N$ graph for b-boson self-energy.

some graphs for the self-energy connecting d to $\mathbf{k}$ [Fig. 2(a)], the self-energy of the k propagator [Fig. 2(b)], and the self-energy of the b boson.

Now the convention for ordering graphs in powers of $1/N$ is normally such that the energy scale should go to a finite limit as $N\rightarrow\infty$. This convention requires that V be defined to be of order $1/\sqrt{N}$.[38-41] Hence it is seen that the boson propagator plus its vertices contains a factor V^2, i.e., a factor $1/N$. Fermion loops carry an m sum, giving a factor N. Diagrams with a given number of boson lines having maximal number of fermion loops are the leading-order ones. It is seen that the tadpole graph in Fig. 2(a) is then the leading-order expression for the k-d self-energy. This means that to leading order the k-d self-energy is a structureless point, which we denote by an open circle. In fact, the tadpole graph is equivalent to a self-consistent equation for the expectation value $\langle b\rangle$ of the b boson.

Of course, $\langle b\rangle$ is not gauge invariant and the expectation value strictly does not exist. This question has been discussed thoroughly by Read.[38] Read found that the correlation function $\langle b(0)b(t)\rangle$ behaves like $|t|^{-1/N}$ at long times, a geometrical behavior showing that b has long-range order in time, and that, moreover, order is approached as $N\rightarrow\infty$; hence $\langle b\rangle$ can be introduced, physical quantities so calculated merely developing $1/N$ corrections from the lack of strict order in b at finite N.

Then, introducing $\langle b\rangle$, we have the mean-field Hamiltonian

$$\begin{aligned}\mathcal{H}' &= \sum_{m}\varepsilon_{\mathbf{k}}c^{\dagger}_{\mathbf{k}m}c_{\mathbf{k}m}+\varepsilon_d\sum_{im}d^{\dagger}_{im}d_{im}\\ &+\sqrt{z}\sum_{\mathbf{k}m}(V_{\mathbf{k}}d^{\dagger}_{im}c_{\mathbf{k}m}e^{i\mathbf{k}\cdot\mathbf{r}_i}+\text{H.c.})\\ &+\sum_{i}(\varepsilon_d-E_1)(z-qN)-\mu N \qquad (3.4)\end{aligned}$$

with the notation $\sqrt{z}=\langle b\rangle$. An equation for the expectation value $\langle b\rangle$ is obtained by differentiating the expectation value of (3.4) with respect to $\langle b\rangle$,[38-41]

$$E_1-\varepsilon_d=N\sum_{\mathbf{k}}\frac{V_{\mathbf{k}}}{\sqrt{z}}\langle d^{\dagger}_{0m}c_{\mathbf{k}m}\rangle . \qquad (3.5)$$

Another equation is obtained by differentiating with respect to ε_d,

$$N\langle d^{\dagger}_{0m}d_{0m}\rangle\equiv n_{0d}=qN-z . \qquad (3.6)$$

The expectation values in (3.5) and (3.6) have to be calculated from the kd and d propagators. The leading N self-energy for the k propagator is given in Fig. 2(b). The kd and d propagators (with the d site at origin) are easily derived from the k propagator by adding $V_{\mathbf{k}}\langle b\rangle/(\omega-\varepsilon_d+is)$ factors. Hence (for retarded propagators at $T=0$)

$$G_{\mathbf{k}}(\omega)=\left[\omega+is-\varepsilon_{\mathbf{k}}-\frac{zV^2_{\mathbf{k}}N_s}{\omega+is-\varepsilon_d}\right]^{-1}, \qquad (3.7a)$$

$$G_{\mathbf{k}d}(\omega)=\frac{(zV^2_{\mathbf{k}})^{1/2}}{(\omega+is-\varepsilon_d)}G_{\mathbf{k}}(\omega) , \qquad (3.7b)$$

$$G_d(\omega)=\sum_{\mathbf{k}}\left[(\omega+is-\varepsilon_d)^{-1}+\frac{zV^2_{\mathbf{k}}G_{\mathbf{k}}(\omega)}{(\omega+is-\varepsilon_d)^2}\right], \qquad (3.7c)$$

where N_s is the number of unit cells in the lattice. Now calculation of the expectation values in (3.5) and (3.6) means integration of the imaginary parts of (3.7b) and (3.7c) summed over $\mathbf{k}$, a process normally requiring complex lattice sums. We may greatly simplify it by introducing a model with $\mathbf{k}$-independent $V_{\mathbf{k}}$, $V_{\mathbf{k}}=V/(N_s)^{1/2}$. Then, defining the Green's function of the unhybridized O band,

$$G^0_{\mathbf{k}}(\omega)=(\omega+is-\varepsilon_{\mathbf{k}})^{-1} ,$$

we have

$$G_{\mathbf{k}}(\omega)=G^0_{\mathbf{k}}\left(\omega-\frac{zV^2N_s}{\omega+is-\varepsilon_d}\right). \qquad (3.8)$$

The densities of states are simply

$$\rho_c(\omega)=-\frac{1}{\pi N_s}\operatorname{Im}\sum_{\mathbf{k}}G_{\mathbf{k}}(\omega)=\rho^0_c\left(\omega-\frac{zV^2}{\omega-\varepsilon_d}\right), \qquad (3.9a)$$

$$\rho_{cd}(\omega)=-\frac{1}{\pi N_s}\operatorname{Im}\sum_{\mathbf{k}}G_{\mathbf{k}d}(\omega)=\rho_c(\omega)\frac{(zV^2/N_s)^{1/2}}{\omega-\varepsilon_d} , \qquad (3.9b)$$

$$\rho_d(\omega)=-\frac{1}{\pi N_s}\operatorname{Im}G_d(\omega)=\rho_c(\omega)\frac{zV^2}{(\omega-\varepsilon_d)^2} . \qquad (3.9c)$$

A very simple model of the unhybridized oxygen band DOS $\rho^0_c(\omega)$ is a square band

$$\rho^0_c(\omega)=(2D)^{-1}\Theta(D-\omega)\Theta(\omega+D) , \qquad (3.10)$$

where $\Theta(x)$ is the step function and (3.10) is DOS per spin per O band (there being two O bands per unit cell, one nonbonding, in the model). If we use (3.10), the renormalized upper and lower band edges ε_+ and ε_- from (3.9a) are

$$\varepsilon^P_{\pm}=\left(\frac{\varepsilon_d\pm D}{2}\right)+P\left[\left(\frac{\varepsilon_d\mp D}{2}\right)^2+zV^2\right]^{1/2} \qquad (3.11)$$

where $P=+1$ for the upper hole band and -1 for the lower.

The DOS in the two oxygen orbitals is then the sum of (3.10) for the unhybridized band and, for the hybridized band, (3.9a). Taking $D=2.4$ eV and $V=2.8$ eV, and Mattheiss's value $\varepsilon_d=0$,[1] the result is compared in Fig. 3 with the density of states in the oxygen orbitals in the Mattheiss calculation.[1] The fit is fair. It suggests that our model, whose essential approximations are the separation into hybrid and unhybridized O bands, and the neglect of the k dependence of $V_{\mathbf{k}}$, is at least as good as any other simple one the authors tried. A more optimal shape for $\rho^0_c(\omega)$ would evidently have tails smoothing out the sharp band edges in (3.10), resulting in more DOS in the wings of the band structure in Fig. 3. Nevertheless, the isotropic $V_{\mathbf{k}}$ model is a crude one. To make up for some of its deficiencies, we shall in the following employ modified parameters $D=2.2$ eV, $V=2.0$ eV, which are found to give better overall agreement with experiment.

With the aid of these relatively strong approximations we can calculate the expectation values (3.5) and (3.6)

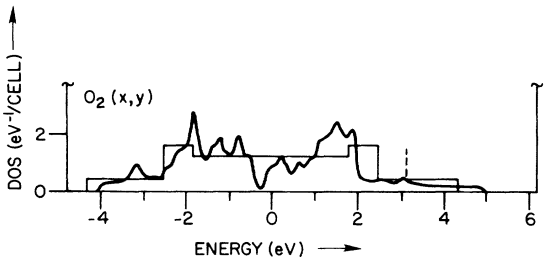

FIG. 3. Density of states of the oxygen p_x,p_y orbitals in the Cu planes in La_2CuO_4. Bold curve, as calculated by Mattheiss (Ref. 1); fine curve, according to the square band model with $D=2.4$ eV, $V=2.8$ eV.

analytically. Equation (3.5) becomes

$$E_1-\varepsilon_d=NV^2\int_{\varepsilon_-}^{\varepsilon_+}\frac{d\omega}{\omega-\varepsilon_d}\frac{1}{2D}f(\omega-\mu)\,, \tag{3.12}$$

where $f(x)$ is the Fermi function. At $T=0$ it gives

$$E_1-\varepsilon_d=\Gamma\ln\left(\frac{\mu-\varepsilon_d}{\varepsilon_--\varepsilon_d}\right), \tag{3.13}$$

where $\Gamma=NV^2/2D$. Equation (3.6) becomes

$$qN-z=\Gamma\int_{\varepsilon_-}^{\varepsilon_+}\frac{d\omega}{(\omega-\varepsilon_d)^2}f(\omega-\mu)\,, \tag{3.14}$$

which at $T=0$ gives

$$qN-z=\Gamma\left(\frac{1}{\varepsilon_--\varepsilon_d}-\frac{1}{\mu-\varepsilon_d}\right). \tag{3.15}$$

Finally, we add a condition on the total number of holes in the system, which from (3.9a) and (3.9c) is

$$N(2D)^{-1}(\mu-\varepsilon_-)+qN-z$$
$$=x_h+1-N(2D)^{-1}(\mu+D)\Theta(\mu+D)\,. \tag{3.16}$$

The last term in (3.16) comes in when μ hits the edge of the nonbonding oxygen $2p$ band. We have already specified the parameters V and D. If we additionally specify E_1 and x_h (the latter controllable in a limited range experimentally), then we may solve (3.13)–(3.16) for μ, ε_d, and z, and calculate other quantities.

In Figs. 4–6 we exhibit results obtained by solving (3.12), (3.15), and (3.16) with $E_1=-3.8$ eV (note this is the one-hole energy) as a function of x_h. In Fig. 4 we show the shift in the self-consistent solution as a function of x_h. First, we note from Fig. 4 that the added holes go mostly into the oxygen orbitals, in agreement with experimental observation.[10] As a result of this, there is little change in the Cu charge with doping, and hence from (3.6) little change in z with doping; z remains near 0.25. Hence the characteristic energy scale $T_K=\varepsilon_d-\mu$ does not change significantly with doping (see Fig. 4). This scale is a measure of the degeneracy temperature in the system, and is seen to lie at around 0.5 eV. We also plot the position $\tilde{E}_2$ of the two-particle resonance associated with the d^8 state, defined in (4.6) below. $\tilde{E}_2$ decreases, i.e., d^8 becomes more accessible, with increasing doping in Fig. 4. The chemical potential goes up with doping, due to hole-hole repulsion.

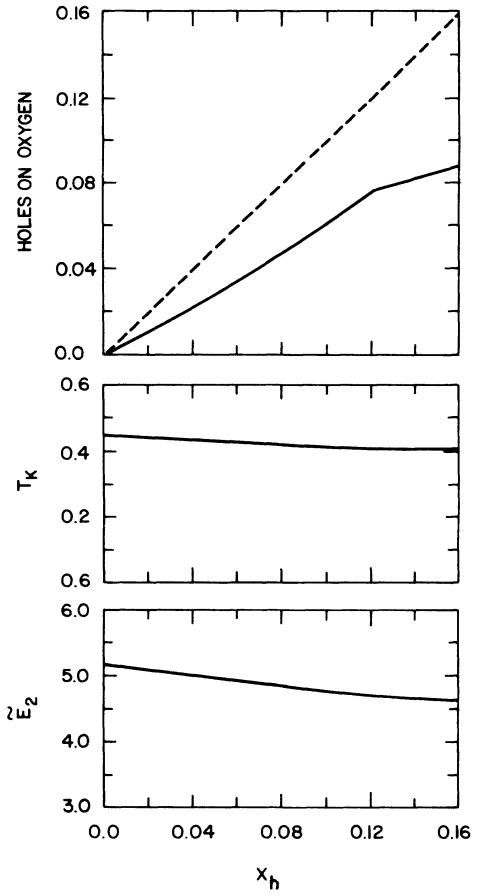

FIG. 4. Self-consistent calculation for normal state in model for $La_{2-x}Sr_xCuO_4$ of various properties vs hole concentration x_h. Top panel, change in hole concentration on oxygen (full curve), broken curve indicates 100% of holes on oxygen. Middle panel, characteristic energy scale $T_K=\varepsilon_d-\mu$; bottom panel, energy $\tilde{E}_2$ of two-particle resonance. Parameters $D=2.2$ eV, $V=2.0$ eV, $E_1=3.8$ eV (electron energy).

The discontinuity in Fig. 4 at $x_h=0.12$ (i.e., 12% doping) in the $La_{2-x}Sr_xCuO_4$ material occurs when, with our parameters, the chemical potential μ hits the top of the nonbonding oxygen band. At this point a further drop in μ with increasing x_h is slowed down. It is incidentally tempting to associate this discontinuity with discontinuity in the Hall coefficient observed.[19,20] Even more speculative, the oxygen loss[20] at $x_h>15\%$ may be associated with the possibility that holes in both the hybridizing and nonhybridizing p orbitals can now go on to oxygen atoms without energy penalty when μ lies in the nonbonding oxygen band. In any case, the region $x_h>0.15$ has been little explored experimentally due to the onset of oxygen loss.[20]

The DOS in the copper plus hybridizing oxygen bands is shown in Fig. 5 for $x_h=0.1$. We have made an electron-hole inversion, so this is the electron DOS. The oxygen part prior to hybridization is shown below the ε

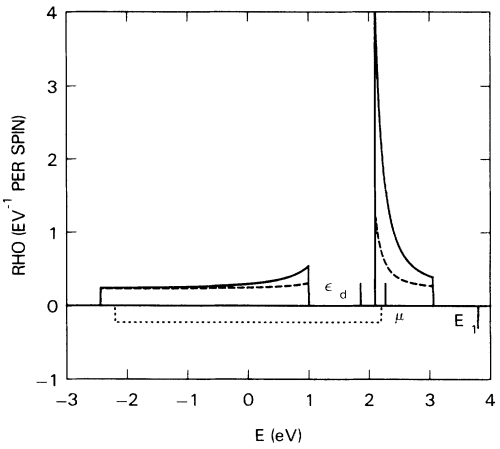

FIG. 5. Self-consistent total density of states in $La_{2-x}Sr_xCuO_4$ per spin vs energy (full curve) for $D=2.2$ eV, $V=2.0$ eV, $E_1=3.8$ eV (electron energy), $x_h=0.1$. Dotted curve is unperturbed oxygen DOS, and broken curve is the projected density of states seen in photoemission in mean-field theory.

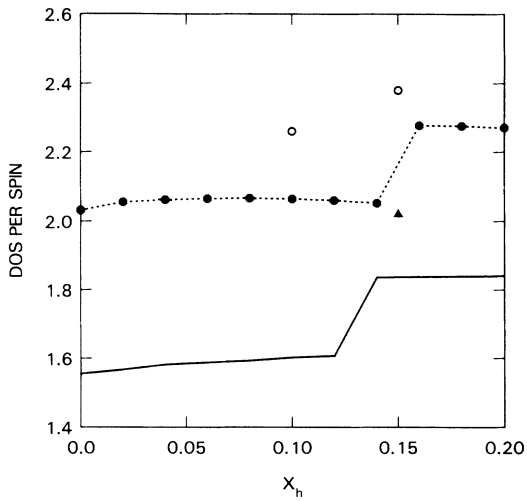

FIG. 6. Total DOS in $La_{2-x}Sr_xCuO_4$ at the Fermi level per spin, plotted vs x_h; curves, as calculated self-consistently with $D=2.2$ eV, $V=2.0$ eV (full curve, $E_1=3.8$ eV; dotted curve, $E_1=4.2$ eV); open circles as deduced from experimental susceptibility (Ref. 9) including core but neglecting Landau corrections; triangle, as deduced from specific-heat jump (Ref. 8) assuming (4.22).

axis, and is just a square band. The effect of hybridization on the oxygen part is not to alter the DOS, but only the band edges. The copper part, however, becomes strongly enhanced, the "heavy-fermion" mass-enhancement effect, in the bottom of the upper band. The quasiparticle DOS at the Fermi level is relatively high.

Photoemission measures, in sudden approximation, the Green's functions of the real electrons,

$$-i\langle Tc_{\mathbf{k}}^{\dagger}(t)c_{\mathbf{k}}(0)\rangle ,$$

and

$$-i\langle TD_{\sigma}^{\dagger}(t)D_{\sigma}(0)\rangle \simeq -iz\langle Td_{\sigma}^{\dagger}(t)d_{\sigma}(0)\rangle , \qquad (3.17)$$

where the approximate result refers to the large-U, mean-field approximation. We illustrate in Fig. 5 the photoemission DOS from (3.17). The occupied states are mostly but not totally Cu-like in the upper band. The photoemission DOS at ε_F is about 1.5 per eV per Cu including spin. Its ratio to the maximum DOS in the combined nonbonding bands in the Mattheiss calculation is around 15%. The photoemission data[21] for $La_{1.8}Sr_{0.2}CuO_4$ show, as expected, that most of the DOS lies in the nonbonding region (from 16 electrons). The DOS in the Fermi-level region is steeply falling with increasing energy, as in Fig. 5, but the measured DOS at ε_F is only 4% of the DOS at the maximum in the nonbonding region. This is less than the theoretical estimate by a factor of about 4. We attribute the discrepancy to surface contamination effects.

The paramagnetic susceptibility χ and linear coefficient of specific heat γ are related to the quasiparticle DOS of Fig. 5 by

$$\chi(0)=2\mu_B^2[\rho_c(\mu)+\rho_d(\mu)]$$

and (3.18)

$$\gamma=\frac{2\pi^2}{3}k_B^2[\rho_c(\mu)+\rho_d(\mu)] .$$

(Incidentally we can show that $D_{i\uparrow}^{\dagger}D_{i\uparrow}-D_{i\downarrow}^{\dagger}D_{i\downarrow}=d_{i\uparrow}^{\dagger}d_{i\uparrow}-d_{i\downarrow}^{\dagger}d_{i\downarrow}$. Hence we can calculate the susceptibility directly from the quasiparticles.) χ is difficult to measure accurately due to comparatively larger diamagnetic corrections,[9] while γ suffers from the uncertainty of being induced from the C_v jump at T_c.[8] Typical values are[9,8] $\chi=1.54\times10^{-4}$ emu/mole and $\gamma=9.5\times10^3$ J/mole for $x=0.15$. These are both compatible via (3.18), with the estimated DOS of $\rho\simeq2$ per eV per spin at ε_F in Fig. 5. In fact, our parameter E_1 was chosen to be compatible with these values.

In Fig. 6 we show the variation of $\chi(0)$ with χ_h. χ is seen to increase slightly with doping, as observed. From the curvature of the DOS in Fig. 5 we would also expect χ to have positive T^2 coefficient: indeed χ does increase slightly with T.[9]

IV. SUPERCONDUCTIVITY

We now need to include the a boson, which is intimately related to superconductivity in our model. To simplify the notation, let us imagine that we have summed over all tadpole graphs [Fig. 2(a)], thus inserting the mean-field corrections due to the b bosons, which are assumed not to vary over $0-T_c$. Let us diagonalize (3.4) to give

$$\mathcal{H}_{\mathrm{MF}}=\sum_{\mathbf{k}m}E_{\mathbf{k}+}C_{\mathbf{k}m+}^{\dagger}C_{\mathbf{k}m+}+\sum_{\mathbf{k}m}E_{\mathbf{k}-}C_{\mathbf{k}m-}^{\dagger}C_{\mathbf{k}m-}+\sum_i(\varepsilon_d-E_1)(z-qN) . \qquad (4.1)$$

In (4.1)

$$E_{\mathbf{k}+}=\varepsilon_d+\langle b\rangle V\tan\theta_{\mathbf{k}} ,$$
$$E_{\mathbf{k}-}=\varepsilon_d-\langle b\rangle V\cot\theta_{\mathbf{k}} , \qquad (4.2)$$

and the new eigenstates represented by the operators $C_{\mathbf{k}m\pm}$ are

$$d_{\mathbf{k}m} = \cos\theta_{\mathbf{k}} C_{\mathbf{k}m+} - \sin\theta_{\mathbf{k}} C_{\mathbf{k}m-} ,$$
$$c_{\mathbf{k}m} = \sin\theta_{\mathbf{k}} C_{\mathbf{k}m+} + \cos\theta_{\mathbf{k}} C_{\mathbf{k}m-} , \tag{4.3}$$

where

$$d_{\mathbf{k}m} = \frac{1}{\sqrt{N_s}} \sum_{\mathbf{k}} e^{i\mathbf{k}\cdot\mathbf{r}_i} d_{im}$$

and

$$\cot(2\theta_{\mathbf{k}}) = \frac{(\varepsilon_d - \varepsilon_k)}{2\langle b\rangle V} . \tag{4.4}$$

In this section we set $\mu \equiv 0$ for simplicity.

We shall see that to the order perturbation theory considered in this paper, superconductivity involves mostly states near the Fermi energy. Then we shall find that only the lower (hole) band, i.e., the upper band in Fig. 5, are important in pairing. We make use of this simplification in rewriting $\mathcal{H}$ in terms of the quasiparticle eigenstates.

Hence writing (3.1) in the representation (4.1)–(4.4) we have (dropping the minus subscript since it is understood that only the lower renormalized band is included)

$$\mathcal{H} = \sum_{\mathbf{k}m} E_{\mathbf{k}} C^{\dagger}_{\mathbf{k}m} C_{\mathbf{k}m} - N_s^{-1/2} \sum_{\mathbf{k}\mathbf{q}m} V g_{\mathbf{k}+\mathbf{q},\mathbf{k}} b^{\dagger}_{\mathbf{q}} C^{\dagger}_{\mathbf{k}m} C_{\mathbf{k}+\mathbf{q}m}$$
$$+ \text{H.c.} - N_s^{-1/2} \sum_{\mathbf{k}\mathbf{q}m} V' g_{\mathbf{k}+\mathbf{q},\mathbf{k}} a^{\dagger}_{\mathbf{q}} C_{\mathbf{k}m} C_{\mathbf{k}+\mathbf{q}m} \operatorname{sgn} m$$
$$+ \text{H.c.} + \tilde{E}_2 \sum_{\mathbf{q}} a^{\dagger}_{\mathbf{q}} a_{\mathbf{q}} + \tilde{E}_0 \sum_{\mathbf{q}} b^{\dagger}_{\mathbf{q}} b_{\mathbf{q}} , \tag{4.5}$$

where

$$g_{\mathbf{k}',\mathbf{k}} = \sin\theta_{\mathbf{k}'} \cos\theta_{\mathbf{k}} .$$

In Eq. (4.5)

$$\tilde{E}_2 = E_2 + \varepsilon_d - E_1 ,$$
$$\tilde{E}_0 = \varepsilon_d - E_1 , \tag{4.6}$$

are (hole) affinity and ionization excitation energies of the d orbital with respect to a "bound state" at $\mu - \varepsilon_d$, and

$$a_{\mathbf{q}} = N_s^{-1/2} \sum_i e^{i\mathbf{k}\cdot\mathbf{r}_i} a_i ,$$
$$b_{\mathbf{q}} = N_s^{-1/2} \sum_i e^{i\mathbf{k}\cdot\mathbf{r}_i} b_i . \tag{4.7}$$

Equation (4.5) is to be employed without including the tadpole diagrams, which are already contained within mean field. Care is necessary when changing values of the mean-field parameters $\langle b\rangle$ and ε_d due to $1/N$ corrections, a procedure not required in this paper.

In the present notation all fermions are represented just by full lines, the relative contributions of the k and d states being taken care of by the coherence factors in the vertices. The sign convention for diagrams containing a bosons is best determined from a t'Hooft-like convention,[42] where the a bosons are represented as two parallel fermion lines of opposite spin but same directionality. The fermion lines entering and leaving the a-boson propagator then pass continuously through it, and whenever they form part of a Fermi loop a -1 factor is produced. Next we consider the formal order in $1/N$ of the a boson. The definition of the a-boson coupling parameter V' differs from that for the b boson by the factor $1/\sqrt{n}$, where $N = 2n$, and thus the a boson becomes $O(1/N^2)$.

The Nambu-Gorkov formalism provides the generalization of the self-energy graphs of Fig. 2(a) to the superconducting phase. The basic equations in a well-known notation are

$$\Sigma(\mathbf{k}, i\omega_n) = i\omega_n (1 - Z(\mathbf{k}, i\omega_n))\tau_0 + Z(\mathbf{k}, i\omega_n)\Delta(\mathbf{k}, i\omega_n)\tau_1 , \tag{4.8}$$

where Σ is the self-energy, τ_0 the 2×2 unit matrix $\tau_{0ij} = \delta_{ij}$, and $\tau_{1ij} = (1 - \delta_{ij})$. Equation (4.8) defines Z and Δ implicitly. From the Dyson equation the fermion Green's function is

$$G^{-1}(\mathbf{k}, \omega_n) = \begin{pmatrix} i\omega_n Z - E_{\mathbf{k}} & -Z\Delta \\ -Z\Delta & i\omega_n Z + E_{\mathbf{k}} \end{pmatrix} , \tag{4.9}$$

while

$$G(\mathbf{k}, \omega_n) = (\det G^{-1})^{-1} \begin{pmatrix} i\omega_n Z + E_{\mathbf{k}} & Z\Delta \\ Z\Delta & i\omega_n Z - E_{\mathbf{k}} \end{pmatrix} , \tag{4.10}$$

and

$$\det G^{-1} = (i\omega_n)^2 Z^2 - E_{\mathbf{k}}^2 - Z^2\Delta^2 . \tag{4.11}$$

Now we write out the diagrams for the self-energy Σ to leading order in $1/N$. The τ_0 part of Σ gives the diagram already considered in Fig. 2(a) [$O(1)$]. In the normal state, together with the condition $\langle n_d\rangle + \langle b^{\dagger} b\rangle = qN$, this gives back the self-consistency equations of Sec. III. We shall assume that they are not significantly altered by superconductivity, an assumption justified by the largeness of the normal-state energy scale $T_K \equiv \mu - \varepsilon_d \sim 0.5$ eV relative to T_c. The leading-N self-energy is frequency independent, hence $Z = 1$.

Before evaluating the diagrams of Fig. 7 for the τ_1 part of the self-energy, we have to address the pseudopotential problem, which arises in considering Fig. 7(b). The contribution [Fig. 7(b)] to the self-energy occurs in the $U = \infty$ model and was treated by Lavagna, Millis, and Lee,[43] and by Houghton, Read, and Won.[44] These authors only consider small energy transfer $|\omega| < T_K$ through the b boson. This on-shell approximation is analogous to the $|\omega| < \omega_D$ approximation in phonon pairing theory, which is motivated by the decay of the

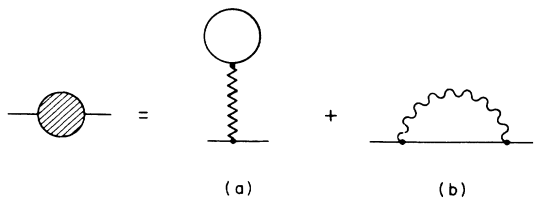

FIG. 7. Order $(1/N)$ diagrams for the anomalous part of the self-energy. Wavy line, b boson; zig zag line, a boson; full line, fermion propagator in the lower heavy-fermion hole band.

phonon propagator in the region $\omega \gg \omega_D$. However, the b boson differs from the phonon propagator[45] in that the propagator does not die away but approaches a constant in the region $T_K < \omega < D$, resembling the Coulomb part of the kernel in phonon-mediated superconductivity. The contributions from the rest of the energy region $D > |\omega| > T_K$ can be included, in the same way as for the Coulomb pseudopotential μ^* in conventional superconductivity, via a pseudopotential. Diagrams for the pseudopotential part of the self-energy involve scattering outside the $|\omega| < T_K$ shell and are shown in Figs. 8(a) and 8(b). They are formally of order $1/N^2$. Note that a difference which the present model has from conventional superconductivity is that here the pseudopotential is attractive, whereas the low-frequency part of Fig. 7(b) is repulsive, canceling part of the attractive term [Fig. 7(a)].

The procedure we adopt for structuring the calculation then assigns these attractive pseudopotential contributions to order $1/N^2$. The contributions we are left with in $O(1/N)$ for the τ_1 part of the self-energy are to be evaluated only with the energy transfer inside the cutoff, $|\omega| < T_K$.

Now in the usual spirit of pseudopotential theory we replace the b boson in Fig. 7(b) by its $\omega=0$ value and s-wave average over the q dependence, when we obtain a contribution to the self-energy

$$-\frac{1}{N\rho}\left[1-\frac{0.2}{N}\right]\sum_{\mathbf{k}'n}\frac{1}{\omega_n^2+E_{\mathbf{k}'}^2+\Delta^2}, \tag{4.12}$$

where ρ is the DOS at the Fermi surface.

The diagram of Fig. 7(a) is the same as already considered in Refs. 28 and 29, and is given by

$$g_{\mathbf{k}\mathbf{k}}\frac{2NV'^2}{\tilde{E}_2}\sum_{\mathbf{k}'n'}g_{\mathbf{k}'\mathbf{k}'}\frac{\Delta(\mathbf{k}',\omega_{n'})}{\omega_{n'}^2+E_{\mathbf{k}'}^2+\Delta^2}. \tag{4.13}$$

Due to the narrowness of the lower hole band, it makes only a very small difference whether we take the lower energy of the $\mathbf{k}'$ sum at $\mu - T_K$ or at the lower band edge, and we choose the latter, as in Refs. 28 and 29.

Equations (4.12) and (4.13) are the contributions to Δ, giving the gap equation

$$\Delta(\mathbf{k},\omega_n)=g_{\mathbf{k}\mathbf{k}}\frac{2NV'^2}{\tilde{E}_2}\sum_{\mathbf{k}'n'}g_{\mathbf{k}'\mathbf{k}'}\frac{\Delta(\mathbf{k}',\omega_{n'})}{\omega_{n'}^2+E_{\mathbf{k}'}^2+\Delta^2}-\frac{1}{N\rho}\left[1-\frac{0.2}{N}\right]\sum_{\mathbf{k}'n'}\frac{\Delta(\mathbf{k}',\omega_{n'})}{\omega_{n'}^2+E_{\mathbf{k}'}^2+\Delta^2}. \tag{4.14}$$

Now in the second term of (4.14) the cutoff for $\mathbf{k}'$ very different from $\mathbf{k}_F$ has been defined in an approximate way. By redefining how the cutoff in this term is done, we may analytically solve the integral equation (4.14) on shell. To do this, we insert an extra factor $g_{\mathbf{k}'\mathbf{k}'}/g_{\mathbf{k}\mathbf{k}}$, which is unity at $\mathbf{k}=\mathbf{k}'=\mathbf{k}_F$, into (4.14), to obtain

$$\Delta(\mathbf{k},\omega_n)=g_{\mathbf{k}\mathbf{k}}\left[\frac{2NV'^2}{\tilde{E}_2}-\frac{1}{N\rho g_{\mathbf{k}_F\mathbf{k}_F}^2}\left[1-\frac{0.2}{N}\right]\right]\times\sum_{\mathbf{k}'n'}g_{\mathbf{k}'\mathbf{k}'}\frac{\Delta(\mathbf{k}',\omega_{n'})}{\omega_{n'}^2+E_{\mathbf{k}'}^2+\Delta^2}, \tag{4.15}$$

where additionally the $\mathbf{k}=\mathbf{k}_F$ approximation has been made in the $g_{\mathbf{k}\mathbf{k}}^2$ factor.

Making the BCS assumption that Δ is independent of ω_n up to the cutoff yields the solution $\Delta(\mathbf{k})=\delta g_{\mathbf{k}\mathbf{k}}$, and the gap equation

$$1=\left[\frac{2NV'^2}{\tilde{E}_2}-\frac{1}{N\rho_0\sin^2\theta_{\mathbf{k}_F}}\left[1-\frac{0.2}{N}\right]\right]\times\sum_{\mathbf{k}'n'}\frac{g_{\mathbf{k}'\mathbf{k}'}^2}{\omega_{n'}^2+E_{\mathbf{k}'}^2+\delta^2 g_{\mathbf{k}'\mathbf{k}'}^2}. \tag{4.16}$$

In (4.16) we have used the identity $\rho_0=\rho\cos^2\theta_{\mathbf{k}_F}$.

The $\mathbf{k}$ sum in (4.16) may be evaluated to logarithmic accuracy (see Appendix A), giving at $T=T_c$

$$T_c=1.14\omega_c\exp\left[-\left[\frac{4V^2\rho_0}{\tilde{E}_2}-\tilde{u}\right]^{-1}\right],\qquad \tilde{u}=\frac{1}{N\rho_0\sin^2\theta_{\mathbf{k}_F}}\left[1-\frac{0.2}{N}\right], \tag{4.17}$$

where $\omega_c^2=\varepsilon^-\varepsilon^+$, and we have set $N=2$, when $\tilde{u}\sim 0.5$. For simplicity, we have assumed $\rho \gg \rho_0$. Equation (4.17) is useful for intuitive purposes, but for numerical evaluation we return to (4.16).

Equation (4.17) shows that the attractive interaction between the quasiparticles responsible for superconductivity is essentially exchange via the d^8 state. This is opposed by the intrinsic quasiparticle-quasiparticle repulsion $\tilde{u}$, which plays the role of μ^* in conventional phonon-mediated superconductivity. It is the near cancellation of these two terms which is responsible for the relatively modest values of T_c, observed in high-T_c superconductors, despite the large values of $\omega_c \sim 1$ eV. We would like to stress here that the value of $\tilde{u}$ is obtained explicitly from our solution in contrast to the empirical nature of the analogous μ^* parameter which appears in conventional

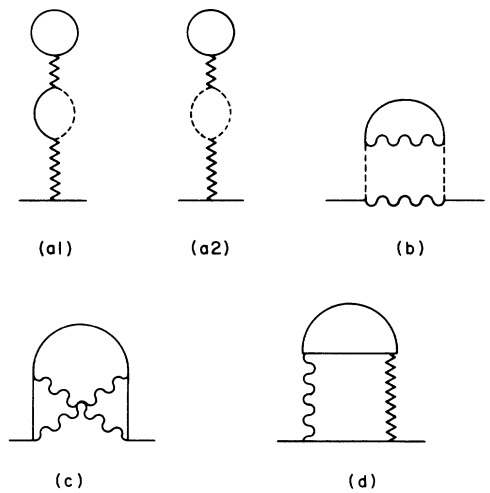

FIG. 8. Order $(1/N^2)$ diagrams for the anomalous self-energy. (a),(b) As for Fig. 7, except that the broken line involves propagator in the upper heavy-fermion hole band. (c),(d) Here full lines represent fermion propagators in both upper and lower bands.

superconductivity.

In Fig. 9 we plot T_c, obtained by solving (4.16) numerically at $T=T_c$, versus hole concentration x_h. The Coulomb repulsion U, which is frequently quoted as being in the range 6.0–6.5 eV (recently the estimates have tended to increase slightly) is taken at $U=5.9$ eV to optimize the fit to the data at one point. In this figure we have taken the density of states in the nonbonding band from our more-accurate calculation (which gives 20 eV^{-1}) and inserted in into the third term in (3.16) instead of $(2D)^{-1}$. It is first seen that the behavior at low x_h, where the $1/N$ expansion can be expected to fail due to dominance by spin fluctuations, is not accurate. However, the trend of T_c to increase with x_h, and to saturate at $x_h \sim 0.14$, is given correctly. The origin of the saturation is simply that when the chemical potential, which lies in the p_σ band, hits the top of the high-DOS nonbonding band, x_h in the p_σ band stabilizes. We interpret the subsequent fall in T_c at $x_h=0.3$ As some kind of extrinsic effect; it is most unlikely that doping in the p_σ band reaches such a high level as 0.3 in this material. As regards the slightly low value of $U=5.9$ eV, we know from the experimental α coefficient[16] that part of the pairing force comes from phonons in the La material. Our calculation compensates for neglecting phonon-mediated attraction by increasing the exchange, and thus decreasing U.

In Fig. 9 we also show the extrapolation of $T_c(x_h)$ if the chemical potential were imagined not to hit the nonbonding band. It is seen that T_c increases rapidly with x_h. We propose that the explanation of higher T_c in other (e.g., 1:2:3) materials may be found in Fig. 9, in terms of their energy-band structure, enabling higher levels of doping to be sustained in the p_σ band without holes getting into the nonbonding band.

The properties of the solution to (4.16) at low temperatures are closely similar to BCS. For $V_{\mathbf{k}}=V$, the gap is of course isotropic. It turns out that even in more realistic models, near isotropy of the gap is retained.

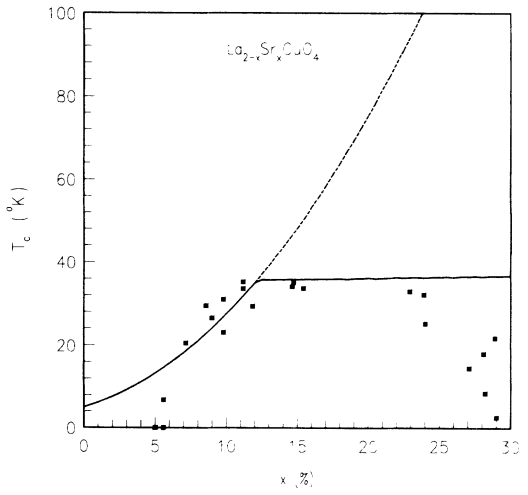

FIG. 9. T_c vs hole concentration x_h. Points, data from Ref. 20 and from Torrance (Ref. 56). Full curve, present model with $U=5.9$ eV, and DOS in the nonbonding band taken from Ref. 49 as 20 eV^{-1}. Dotted curve, extension and results assuming that hole concentration in the p_σ band above $x_h=0.12$ continued to be given by x_h.

At $T=0$, the $\mathbf{k}$ sum in (4.16) is again calculated to logarithmic accuracy (Appendix A). Comparing (A6) and (A10), we retrieve the BCS result

$$2\Delta=3.5k_BT_c\,, \tag{4.18}$$

where $\Delta=g_{\mathbf{k}_F\mathbf{k}_F}\delta$. The result (4.18) is confirmed by numerical solution of (4.16) both at $T=T_c$ and at $T=0$. Result (4.18) is essentially inevitable given that the two-particle scattering kernel associated with Fig. 7 is frequency independent until the very-high-energy cutoff T_K is reached.

Similarly, the specific-heat jump may be calculated by the methods given in Sec. V, and gives

$$\Delta C_V=1.43\gamma T_c\,, \tag{4.19}$$

again the BCS result. The critical field is also found to take essentially the BCS value

$$H_c\simeq(4\pi v^{-1}\rho)^{1/2}\,, \tag{4.20}$$

where v is the volume per Cu atom.

One effect of pressure is to induce approximately equal but opposite changes in the energies of the d^8 and d^{10} states relative to the d^9 state. We expect

$$E_1\rightarrow E_1-\delta,\quad U\rightarrow U\,, \tag{4.21}$$

where $\delta=\alpha p$, and $\alpha>0$. The strongest effect of δ on T_c is expected to be in decreasing $\tilde{E}_2$ by δ, thus increasing T_c. Pressure should also increase χ by decreasing T_K, and thus increasing $|E_1|$. Now we may define a quantity γ' which for small pressures is independent of the unknown coefficient α,

$$\gamma'=(\Delta T_c/T_c)/(\Delta\chi/\chi)\,. \tag{4.22}$$

The quantity γ' may be calculated numerically from our formulation, giving $\gamma'=5.8$ at $x_h=0.13$. an experimental determination gives $\gamma'=3.9$. We expect our estimate to be too large because of the neglect of phonons, which do not couple to pressure in the manner we describe.

A remarkable feature of the present formulation of high-T_c superconductivity is its intimate relationship with a-boson dynamics. In fact, the phase transition at T_c is signaled by a divergence in the a-boson propagator. This may be inferred from the form (2.18) for the order parameter, which suggests that $|a|$ might diverge at T_c. More explicitly, the diagrams for the two-particle propagator may be rearranged into the series for the a-boson propagator (Fig. 10). Hence a divergence in the two-particle propagator at T_c implies that the a-boson propagator becomes soft at T_c. We see that as T is lowered, first the b boson becomes soft at T_K, then the a boson becomes soft at T_c. Is superconductivity then a Bose condensation in the present theory?

In the next section we calculate the critical properties of the model in terms of the a-boson field, and show that the critical region is narrow, resembling superconductivity rather than superfluidity. However, due to special features of the present systems, e.g., the high T_c and the high mass along the z direction, the critical region is pre-

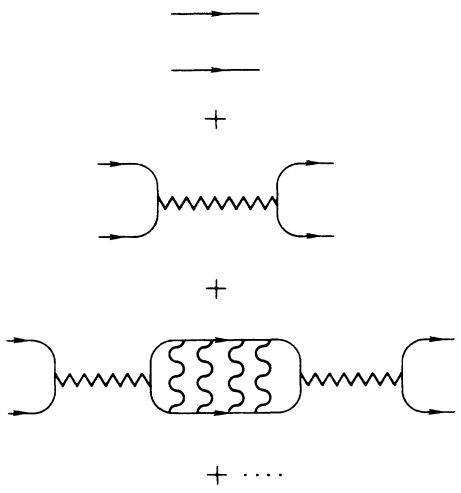

FIG. 10. Rearrangement of diagrams for the two-particle propagator as a series for the a-boson propagator.

dicted to be observable, with width ~ 1 K, in agreement with recent data.

V. CRITICAL FLUCTUATIONS

The various mechanisms for the formation of a superconducting condensation generally imply a specific structure of the many-body Hamiltonian. The parameters of such a Hamiltonian predict, for example, a specific critical temperature T_c. For the Hamiltonian discussed in the preceding section, T_c in the weak-coupling limit is given in Eq. (4.17) in terms of the basic entries to the original Hamiltonian in Eq. (2.7). These are V, E_1, E_2, x_h, μ, and ρ_0, which is the density of states at the Fermi surface for the dispersion $\varepsilon_{\mathbf{k}}$. However, a second feature which goes in tandem with the prediction of the critical temperature is the width of the critical region around T_c. Here we calculate this region for the Hamiltonian of Eq. (2.7) in the weak-coupling limit in terms of the same basic parameters. We also discuss in Appendix B the possibility of more-complex order parameters than the two-component xy model of Eqs. (2.7) or (2.10), and their implication in the critical region. It is important to carry out such calculations since they provide further restrictions to the type of Hamiltonians which successfully predict both measurable quantities, T_c and the critical fluctuations around T_c. Since in high-T_c superconductors (and perhaps also in superconductivity of the heavy fermions) κ (i.e., the Landau-Ginsburg parameter) is very large (100) and the Cooper pair size is relatively small ($\xi_0 \simeq 50$ Å; both κ and ξ_0 are very anisotropic), the critical region should be observable and should therefore provide an important additional guide to the microscopic structure of the Hamiltonian.

In this section we show that even if the critical properties are discussed in terms of a bosons, whose propagator diverges at T_c, the width of the critical region is narrow (but observable) in contrast to the properties of a Bose gas. Rigorously, the following discussion in terms of a bosons is based on the $1/N$ counting of Ref. 28. In this technique only Fig. 7(a) is to leading order, and the a-boson expectation value $\langle a \rangle$ is nonzero for $T < T_c$. To leading order in $1/N$ the quantity $\tilde{u}$ is zero. Nevertheless, the only effect of the introduction of $\tilde{u}$ is to rescale T_c, which may then be assumed to take its experimental value.

We first write the partition function for Eq. (2.7) in a functional integral form,[38] i.e.,

$$Z = \int_{-\pi/\beta}^{\pi/\beta} \prod_i \left(\frac{\beta d\lambda_i}{2\pi} \right) \int DbDb^{\dagger} DaDa^{\dagger} DdDd^{\dagger} DcDc^{\dagger} \times \left[\exp\left(-\int_0^{\beta} d\tau L(\tau) \right) \right], \tag{5.1a}$$

where

$$\begin{aligned} L(\tau) = & \sum_i b^{\dagger}(\mathbf{r}_i) \left(\frac{d}{d\tau} + E_0 \right) b(\mathbf{r}_i) + \sum_i a^{\dagger}(\mathbf{r}_i) \left(\frac{d}{d\tau} + E_2 \right) a(\mathbf{r}_i) \\ & + \sum_{i\sigma} d_{\sigma}^{\dagger}(\mathbf{r}_i) \left(\frac{d}{d\tau} + E_1 \right) d_{\sigma}(\mathbf{r}_i) + \sum_{\mathbf{k}\sigma} c_{\mathbf{k}\sigma}^{\dagger} \left(\frac{d}{d\tau} + \varepsilon_{\mathbf{k}} \right) c_{\mathbf{k}\sigma} + \sum_{\mathbf{k}\sigma i} [V_{\mathbf{k}} b(\mathbf{r}_i) d_{\sigma}^{\dagger} c_{\mathbf{k}\sigma} e^{i\mathbf{k}\cdot\mathbf{r}_i} + \text{H.c.}] \\ & + \sum_{\mathbf{k}\sigma i} [V_{\mathbf{k}} a^{\dagger}(\mathbf{r}_i) d_{\sigma} c_{\mathbf{k}\sigma} e^{i\mathbf{k}\cdot\mathbf{r}_i} \operatorname{sgn}\sigma + \text{H.c.}] + i \sum_{i\sigma} \lambda_i [d_{\sigma}^{\dagger}(\mathbf{r}_i) d_{\sigma}(\mathbf{r}_i) + b^{\dagger}(\mathbf{r}_i) b(\mathbf{r}_i) + a^{\dagger}(\mathbf{r}_i) a(\mathbf{r}_i) - 1] . \end{aligned} \tag{5.1b}$$

In Eq. (5.1), D is shorthand for $\prod_{i\sigma} Dd_{\sigma}(\mathbf{r}_i), \ldots$, etc. In the functional integral form of Eq. (5.1) the integral over $c_{\mathbf{k}\sigma}$ and $d_{\sigma}(\mathbf{r}_i)$ are anticommuting and $b(\mathbf{r}_i)$ and $a(\mathbf{r}_i)$ commuting complex Grassman numbers. The additional integrals over λ_i ensure that the constraint in Eq. (2.3) is satisfied.

We next take Eq. (5.1) and develop a corresponding Landau-Ginsburg (LG) free-energy density expansion for $a(\mathbf{r}_i)$ to get

$$\begin{aligned} \beta f(\mathbf{x}) = & \sum_{\alpha} \tfrac{1}{2} a_1 [a_1^2(\mathbf{x}) + a_2^2(\mathbf{x})] + \tfrac{1}{2} a_2 \left[[\nabla_{\parallel} a_1(\mathbf{x})]^2 + \gamma^2 \left(\frac{\partial}{\partial z} a_1(\mathbf{x}) \right)^2 + [\nabla_{\parallel} a_2(\mathbf{x})]^2 + \gamma^2 \left(\frac{\partial}{\partial z} a_2(\mathbf{x}) \right)^2 \right] \\ & + a_3 [a_1^4(\mathbf{x}) + a_2^4(\mathbf{x}) + 2a_1^2(\mathbf{x}) a_2^2(\mathbf{x})] \end{aligned} \tag{5.2a}$$

and

$$Z \equiv e^{-\beta F} = \int Da(\mathbf{x}) \exp\left[-\beta \sum_{\mathbf{x}} (f(\mathbf{x})\right]. \tag{5.2b}$$

Here we took the continuum limit of $\mathbf{r}_i \rightarrow \mathbf{x}$ and $\mathbf{x} \equiv \mathbf{x}_{\parallel}, z$. The subscripts 1 and 2 in Eq. (5.2a) are the real and imaginary components of $a(\mathbf{x})$; $a(\mathbf{x}) \equiv a_1(\mathbf{x}) + i a_2(\mathbf{x})$. The critical region of Eq. (5.2) corresponds then to the universality class of an isotropic two-component Heisenberg model (i.e., the x-y model). The anisotropy in the spatial dimension z is given by γ and represents the large anisotropy in the mass in the plane $\mathbf{x}_{\parallel}$ and perpendicular to it along z (i.e., c axis) (see below).

The coefficients α_1, α_2, and α_3 of Eq. (5.2a) can now be calculated by making a free-energy expansion[44] of Eq. (5.2b) to fourth order in $a(\mathbf{q})$ (see Fig. 11) using the diagonalized form given in Eq. (4.5). Also, around the phase transition line of $\langle a^{\dagger}(\mathbf{q}) \rangle$ we expect the quantum fluctuations in $a(\mathbf{q})$ to be unimportant and we can ignore the term $a^{\dagger}(\mathbf{q})(\partial/\partial\tau)a(\mathbf{q})$ in Eq. (5.1) and replace the Bose operator by a classical complex number $a(\mathbf{q})$. Then

$$f = \sum_{\alpha,q} \{[E_2 + \lambda + \kappa_2(\mathbf{q},T)][a_1^2(\mathbf{q}) + a_2^2(\mathbf{q})]\} + \kappa_4(T) \sum_{\alpha,\mathbf{x}} [a_1^4(\mathbf{x}) + a_2^4(\mathbf{x}) + a_1^2(\mathbf{x}) a_2^2(\mathbf{x})], \tag{5.3a}$$

where

$$\kappa_2(\mathbf{q},T) = \frac{1}{\beta} \sum_{\mathbf{k}\xi_1} v^2(\mathbf{k}) \frac{1}{[\xi_1 - E(\mathbf{k}-\mathbf{q})]} \frac{1}{[\xi_1 + E(\mathbf{k})]} \tag{5.3b}$$

and

$$\kappa_4(T) = \frac{1}{2\beta} \sum_{\mathbf{k}\xi_1} v^4(\mathbf{k}) \frac{1}{[\xi_1 - E(\mathbf{k})]^2} \frac{1}{[\xi_1 + E(\mathbf{k})]^2}, \tag{5.3c}$$

where $E(\mathbf{k})$ is defined in Eq. (4.2), $V(\mathbf{k}) = \sin(2\theta_{\mathbf{k}})V$, and the sum over ξ_1 are the usual Matsubara sums. The critical temperature T_c is then given by

$$\kappa_2(0,T_c) = E_2 + \lambda \equiv E_2 - E_1 + \varepsilon_d. \tag{5.4a}$$

α_1 and α_2 are related to two different expansions of $\kappa_2(\mathbf{q},T)$: α_1 is the expansion of $\beta\kappa_2(\mathbf{q}=0,T)$ around T_c, i.e.,

$$\tfrac{1}{2}\alpha_1 = \beta_c \frac{\partial}{\partial T} \kappa_2(\mathbf{q}=0,T)_{T=T_c}(T - T_c). \tag{5.4b}$$

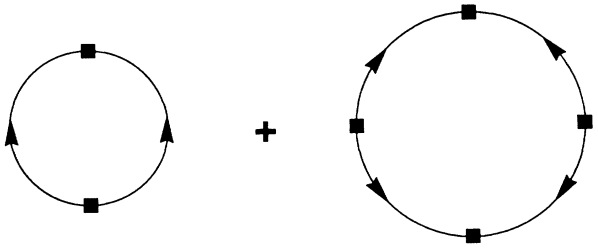

FIG. 11. Free-energy contribution of Eq. (5.3) to fourth order in the Bose fields $a_{\mathbf{q}}$. The filled squares are the Bose fields $a_{\mathbf{q}}$ and the arrowed lines the "heavy-fermion" propagators $\langle C_{\mathbf{k}m}^{\dagger} C_{\mathbf{k}m} \rangle$.

α_2 is the expansion of $\beta_c\kappa_2(\mathbf{q},T=T_c)$ around $\mathbf{q}=0$, i.e.,

$$\alpha_2 = \beta_c \frac{\partial^2}{\partial q^2} \kappa(\mathbf{q}^2,T_c)_{\mathbf{q}=0}. \tag{5.4c}$$

Finally, the quartic coefficient α_3 is

$$\alpha_3 = \beta_c \kappa_4(T_c). \tag{5.4d}$$

The Matsubara sums are trivially performed. What about the sum over $\mathbf{k}$? Unlike most properties discussed in the preceding sections, the critical region depends crucially on the large mass anisotropy. The coupling of the various mass components turn the critical region into clearly a three-dimensional system. We, therefore, must account for the dispersion of $E_{\mathbf{k}}$, or more precisely $\varepsilon_{\mathbf{k}}$, along the c axis. A very reasonable approximation for $\varepsilon_{\mathbf{k}}$ is

$$\varepsilon_{\mathbf{k}} \simeq \varepsilon_{\mathbf{k}_{\parallel}} + \frac{\mathbf{k}_z^2}{2m_z}. \tag{5.5a}$$

In order to determine the α_2 term [Eq. (5.4c)] analytically, we further approximate $\varepsilon_{\mathbf{k}}$ by

$$\varepsilon_{\mathbf{k}} \simeq \frac{\mathbf{k}_{\parallel}^2}{2m} + \frac{\mathbf{k}_z^2}{2m_z} \tag{5.5b}$$

(the critical region will not depend very strongly on these approximations). Because of the very large gap at the zone boundary at $G/2$, along the z direction, $\mathbf{k}_z$ is terminated at $G/2$. Finally, since $m \ll m_z$ the shape of the Fermi surface (FS) is assumed to be cylindrical. The sums over $\mathbf{k}$ then give, for α_1, α_2, α_3,

$$\alpha_1 = \frac{(2bV^2)^2 \rho_0 t}{[(bV)^2 + \varepsilon_d^2] T_c}, \tag{5.6a}$$

$$\alpha_2 = 0.033 \frac{3}{4} \frac{\pi\rho_0 P_F^2}{T_c^3} \frac{(2bV^2)^2 \varepsilon_d^4}{[(bV)^2 + \varepsilon_d^2]^3}, \tag{5.6b}$$

$$\alpha_3 = \frac{0.0495}{2} \frac{\pi\rho_0 P_F^2}{T_c^3} \frac{(2bV^2)^4 \varepsilon_d^2}{[(bV)^2 + \varepsilon_d^2]^3}, \tag{5.6c}$$

and

$$\gamma^{-1} \simeq \sqrt{3/2} \frac{m_z}{m} \frac{G}{P_F}. \tag{5.6d}$$

In Eq. (5.6), $t = (T - T_c)/T_c$, ρ_0 is the density of states for the cylindrical FS of Eq. (5.5) per two spins, and P_F is the Fermi momentum perpendicular to the z direction. By making a small $\mathbf{q}$ expansion of $\kappa_2(\mathbf{q},T)$ we must introduce a cutoff on the $\mathbf{q}$ vectors. This cutoff Λ reflects the range of $\kappa_2(\mathbf{q},T)$. From Eq. (5.3b) we find

$$\Lambda_{\alpha} = C \frac{T_c}{P_F} m_{\alpha} \left[\frac{(bV)^2 + \varepsilon_d^2}{\varepsilon_d^2} \right], \tag{5.6e}$$

where C is some constant of order unity. Our description of the critical region will, however, not depend on its precise value. Λ_{α} are the two cutoffs depending on the two directions. The differences in the two cutoffs will, however, not affect the critical region and we drop the index α.

It is important to appreciate this Λ cutoff. The initial microscopic Hamiltonian of Eq. (2.7) correlated the state E_2, of the two electrons, over a lattice distance. It is, how-

ever, wrong to then think of the size of the bound Cooper pairs as in anyway related to this length scale. The size of the Cooper pairs, or more generally the entities making up the order parameter a, corresponds more closely to Λ^{-1}. If the size of the pair is smaller than the interpair distance, then Λ^{-1} is closely related to this interpair distance (this is so in ^{4}He).[46] If the opposite is true (this is generally the case in a superconductor condensate) then Δ^{-1} is closely related to the pair size, or so-called pair correlation length ξ_0.

We return to Eq. (5.2a) and perform two-scale transformations. First, we define $\psi \equiv 2bV^2 a$. Then

$$\beta_c f = \sum_{\mathbf{q}}^{\Lambda} \tfrac{1}{2}[\alpha_1' + \alpha_2'(\mathbf{q}_\parallel^2 + \gamma^2 q_z^2)]\psi(\mathbf{q})\cdot\psi(\mathbf{q}) + \frac{\alpha_3'}{L^d}\sum_{\mathbf{q}_1\mathbf{q}_2\mathbf{q}_3}^{\Lambda}[\psi(\mathbf{q}_1)\cdot\psi(\mathbf{q}_2)] \times[\psi(\mathbf{q}_3)\cdot\psi(-\mathbf{q}_1-\mathbf{q}_2-\mathbf{q}_3)], \tag{5.7}$$

where d is the spatial dimension, ψ has two components $\psi \equiv (\psi_1, \psi_2)$, and $\alpha_1 = \alpha_1'(2bV^2)^2$, $\alpha_2 = \alpha_2'(2bV^2)^2$, $\alpha_3 = \alpha_3'(2bV^2)^4$. The second transformation scales all lengths by λ and redefines $\psi = \phi/(\alpha_2')^{1/2}\Lambda$. After also redefining $\gamma q_z \to q_z$, Eq. (5.7) now takes the form

$$\beta_c f = \sum_{\mathbf{q}}^{\Lambda_0} \tfrac{1}{2}[r(0) + q^2]\phi(\mathbf{q})\cdot\phi(\mathbf{q}) + \frac{u(0)}{L_0^d}\sum_{\mathbf{q}_1\mathbf{q}_2\mathbf{q}_3}^{\Lambda_0}[\phi(\mathbf{q}_1)\cdot\phi(\mathbf{q}_2)] \times[\phi(\mathbf{q}_3)\cdot\phi(-\mathbf{q}_1-\mathbf{q}_2-\mathbf{q}_3)], \tag{5.8a}$$

where

$$r(0) = C_1\left[\frac{(bV^2)^2+\varepsilon_d^2}{\varepsilon_d^2}\right]^2\left[\frac{T_c}{\Lambda}\right]^2\left[\frac{m}{P_F}\right]^2 t, \tag{5.8b}$$

and

$$u(0) = C_2\gamma^{-1}\left[\frac{(bV^2)^2+\varepsilon_d^2}{\varepsilon_d^2}\right]^3\left[\frac{T_c^3}{\rho_0}\right]\left[\frac{m}{P_F}\right]^4\Lambda^{d-4}. \tag{5.8c}$$

where

$$C_1 = 8/3\times 0.066, \quad C_2 = [0.05/(0.066)^2]\times 2\times(\tfrac{4}{3})^2$$

[these coefficients came from the coefficients in Eq. (5.6)]; $\Lambda_0 = L\Lambda$. The scaled free energy in Eq. (5.8a) is precisely the form studied extensively by Rudnick and Nelson.[47] They developed crossover functions which provide a detailed description of the critical region to first order in $\varepsilon \equiv 4-d$.

Very briefly, the idea is to solve the flow of $r(0)$ and $u(0)$ under the renormalization-group (RG) transformations, to lowest order in ε and $u(0)$. These flow equations for Eq. (5.8a) are

$$\frac{dr(l)}{dl} = 2r(l) + \frac{Au(l)}{1+r(l)} \tag{5.9a}$$

and

$$\frac{du(l)}{dl} = \varepsilon u(l) + \frac{Bu^2(l)}{[1+u(l)]^2}, \tag{5.9b}$$

where $A = 4(N+2)K_4$, $B = 4(N+8)K_4$, $K^{-1} = 8\pi^2$, and the coarse graining is given by l. With the initial boundary condition $r(l=0) = r(0)$ and $u(l=0) = u(0)$ [where $r(0)$ and $u(0)$ are given in Eq. (5.8)], Eq. (5.9) can be solved. For large enough l, $r(l)$ is driven away from the critical line and the partition function Z, or equivalently F, can be then derived by standard perturbation expansion. The results for the free energy $F^>$ above T_c are[47]

$$\beta_c F^> = L_0^d\frac{N}{4(d-2)\gamma}\left[K_4\{\ln[1+t(0)]+t(0)-t^2(0)\ln[t(0)]\} + \frac{t^2(0)}{2u(0)(N-4)}\left[Q(l)^{(4-N)/(N+8)}-1\right]\right]. \tag{5.10a}$$

For $T < T_c$,

$$\beta_c F^< = L_0^d\frac{1}{\gamma}\left[\frac{K_4 N t(0)}{2(d-2)} + \frac{t^2(0)}{4u(0)(N-4)}\left[Q(l)^{(4-N)/(N+8)} - \frac{N}{4}\right]\right], \tag{5.10b}$$

where

$$t(0) = r(0) + \tfrac{1}{2}Au(0), \tag{5.10c}$$

$$Q(l) = 1 + \frac{Bu(0)}{\varepsilon}(e^{\varepsilon l}-1). \tag{5.10d}$$

Finally, the number of coarse-graining steps (l) are given by[47]

$$t(0)e^{2l}/Q(l)^{(N+2)/(N+8)} = 1. \tag{5.10e}$$

Incidentally, for technical reasons[47] $\beta_c F^<$ was not previously derived for general N using the flow equations (11a) and (11b). Our results agree with field-theoretic calculations.[48]

To order ε, Eq. (5.10) gives a detailed description of the critical region for the free energy of Eq. (5.8) [or equivalently Eq. (5.2)] in terms of the basic parameters V, E_1, E_2, x_h, and μ of the microscopic Hamiltonian Eq. (2.7) (T_c is a function of these parameters). To implement it we only need to eliminate l in Eq. (5.10e) in favor of $t(0)$ and introduce the results in Eqs. (5.10a) and (5.10b). This can, in general, be done numerically; we delay such a calculation to when finer experimental data of this critical region becomes available. Here we take the simpler task of discussing only the width of the critical region using the Landau-Ginsberg-like criterion. A common way of identifying the critical region is to measure the specific heat $C_v = \partial^2 F/\partial t^2$. For the critical region to be observable it needs to dominate the common classical

jump in C_v below and above T_c; this is the LG criterion. From Eq. (5.10), the jump in C_V is given by

$$\Delta C_v = \frac{1}{16u(0)} \frac{\partial^2}{\partial t^2}[t^2(0)] . \tag{5.11a}$$

The critical fluctuation contribution is given by

$$C_v = \frac{-1}{8u(0)} \frac{\partial^2}{\partial t^2}\{t^2(0)[Q(l)^{2/5}-1]\} , \tag{5.11b}$$

and the LG criteria for the fluctuation to dominate the jump is

$$C_v/\Delta C_v > 1 . \tag{5.11c}$$

Then, using Eq. (5.10), we get the region of temperature where Eq. (5.11c) is satisfied as

$$t < C_3 \left[\frac{P_F}{G}\right]^2 \gamma^{-2} \left[\frac{T_c}{\varepsilon_F}\left[\frac{\varepsilon_d^2+b^2V^2}{\varepsilon_d^2}\right]^{1/2}\right]^4 , \tag{5.12}$$

where $C_3 \simeq (10\times 2^{15})/3^3$ and is related to the coefficients C_1 and C_2 in Eq. (5.8), $\varepsilon_F = P_F^2/2m$. Inside this region C_v carries the exponents of a two-component isotropic Heisenberg model; i.e., $C_v \simeq t^{-a}$, where

$$a = \frac{1}{2} + \frac{(4-N)\varepsilon}{2(N+8)}, \quad N=2 .$$

With the accepted value of $\gamma^{-1} \simeq m_z/m \simeq 50$,[17] $T_c = 100$ K and $\varepsilon_F \simeq 2$ eV, and mass enhancement $[(\varepsilon_d^2+b^2V^2)/\varepsilon_d^2]^{1/2} \simeq 5$, we get a critical region of 1 K, in very good agreement with the latest experimental observations.[15] The most exciting aspect of this result is that each feature, believed to be unique to high-T_c superconductivity, plays a crucial role in Eq. (5.12). To be specific, without mass anisotropy we would be off by $\simeq 10^3$, and without mass enhancement we would be off by $\simeq 25$.

VI. CONCLUSION

This paper considers a model of high-T_c materials in which there is both electron hopping from Cu to oxygen, and from oxygen to oxygen, with a large Coulomb repulsion U on the Cu atom (Anderson lattice model). We solve it by the $1/N$ expansion technique, where $N=2$ is the degeneracy of the d^9 state, working in this paper only to leading order in $1/N$. Pairing is assumed to be s wave.

At this relatively crude, but physical, level of approximation, a remarkably good account of the basic experimental features of these systems is obtained. The normal state is described as a heavy-fermion fluid with a mass enhancement $m^*/m \sim 8$ (though $\langle b\rangle^2 = 4$). Features of the normal state which are described correctly include the paramagnetic susceptibility and linear coefficient of specific heat, and the fact that most of the weight of added holes is on oxygen, while the states at ε_F are mostly d-like. Treatment of a much more accurate model by Papaconstantopoulos and the present authors[49] confirms the present results. Miyakawa and Nagaoka[50] have shown that the heavy-fermion state is also consistent with the Hall coefficient. As regards superconducting properties, the value of T_c and its variation with doping is satisfactorily reproduced, as is the width of the critical region. The gap-to-T_c ratio, however, has the BCS value, a disagreement with the data which is currently being investigated.

A unique feature of our description of high-T_c superconductivity is the role of the a boson, which describes the d^8 state. This boson becomes soft at T_c, as if for a Bose condensation, even though the narrow Ginzburg region is instead typical of superconductivity. The change in weight of the d^8 state at T_c is only about 1/1000, however,

The adjustable parameter we have used is the value of the "oxide gap," the $d^9p^6 \rightarrow d^{10}p^5$ excitation energy. Defined from the center of the O band, our value (3.8 eV) lies in the range of estimates by Schluter and Hybertson,[51] and by Stechel and Jennison,[52] but a lower value has been proposed from calculations by McMahan, Martin, and Satpathy.[53] The value of U, 5.9 eV, is slightly below the range 6–6.5 eV favored by some experimentalists. This is to be expected because of our neglect of the contribution of phonons to pairing, which is significant in the La material.

Calculation of the effects of higher-order diagrams, such as those illustrated in Fig. 8 for the $1/N^2$ corrections to the anomalous self-energy, is highly desirable. In the present formulation, the ultraviolet corrections noted by Houghton and Sudbo[54] form part of this calculation.

Pauling resonating-valence-bond (RVB) theory and many other (e.g., bag model[55]) proponents have worked with the reduced model (Hubbard model) which projects out both the oxygen and d^8 subspaces, replacing them respectively by direct Cu-Cu hopping and by exchange. We do not, of course, know the exact solution of either model, but within the present approximation we notice significant differences between the full and reduced models.

(i) The Hubbard model, even if interpreted in terms of Wannier (mixed Cu and oxygen) orbitals, is not consistent with the duality that added holes go into oxygen, but states at the Fermi surface are mostly Cu-like.

(ii) Because the hole concentration on the Cu changes little with doping, the energy scale T_K in the two-band model is almost doping independent, whereas it is proportional to doping in the Hubbard model. The former result is consistent with the observed susceptibility.

(iii) The variation of the $d^9 \rightarrow d^8$ excitation energy $\tilde{E}_2$ plays an important role in establishing the trend of T_c in this paper, but there is no such trend in the quantity which depends on it, exchange, within the one-band model.

(iv) Attractive diagrams of order $1/N^2$ [Figs. 8(a) and 8(b)] are missing in the Hubbard model.

These differences between the full and reduced models may be irrelevant in discussing generics such as topological (e.g., whether Bose or Fermi statistics) properties, or phenomena depending on dimensionality, but their neglect is seen to be dangerous at a more detailed level.

The most dramatic distinction between the RVB and the Fermi-liquid formulations is that RVB works with separate "holon" and "spinon" degrees of freedom. The holon concentration equals doping x_h, in contrast to the Fermi liquid whose Fermi surface contains $1+x_h$ holes (Luttinger theorem). It is not yet clear whether the formulations are equivalent. Even if they are, explanations of, e.g., the dependence of the Hall coefficient and T_c on x_h may eventually emerge more naturally in terms of

holons.

We comment briefly on the interpretation of T_c variations between different materials which emerges from the picture proposed here. An important limiting factor on T_c is found to be the saturation of doping in the p_σ orbitals because of the onset of hole transfer into other bands. We suggest that the essential difference between the 1:2:3 and 2:1:4 materials is the delayed onset of this saturation, allowing the 1:2:3 materials to reach a higher hole concentration, and hence a higher T_c. An important role in our theory is played by the mapping between the a boson and the order parameter, and thus by the singlet nature of d^8 state. This is in practice due to crystal-field splitting, and we think that at least one role of the planar structure is related to the requirement for a strong tetragonal crystal-field splitting. This suggests a speculation on the new $Ba_{1-x}K_xBiO_3$ material. Let us suppose it is analogous to the Cu materials but involved $s^0-s^1-s^2$ fluctuations, instead of $d^{10}-d^9-d^8$ fluctuations. Bi satisfies the requirement that s^0 and s^2 be both singlets even in a cubic field, whereas Cu requires the strong tetragonal crystal field. Hence $KBiO_3$ can be cubic within the present mechanism, as it is.

ACKNOWLEDGMENTS

This research was sponsored by the Division of Materials Sciences, U.S. Department of Energy under Contract No. DE-ACOS-84OR21400 with Martin Marietta Energy Systems, Inc. We are grateful to many colleagues, in particular to R. L. Greene, F. J. Himpsel, P. M. Horn, A. Houghton, D. H. Lee, A. P. Malozemoff, T. Penney, M. Ronay, M. W. Shafer, and B. Sudbo for valuable discussions.

APPENDIX A

In this appendix we wish to evaluate various $\mathbf{k}$ sums to logarithmic accuracy, starting with

$$S=\frac{1}{4N_s}\sum_{\mathbf{k}}\frac{\sin^2(2\theta_{\mathbf{k}})}{E_{\mathbf{k}}}\tanh\frac{\beta E_{\mathbf{k}}}{2}, \tag{A1}$$

where $E_{\mathbf{k}}$ is given by $E_{\mathbf{k}-}$ in (4.2). We note that $dE_{\mathbf{k}}/d\varepsilon_{\mathbf{k}}$ is from (4.2) and (4.4),

$$\frac{dE_{\mathbf{k}}}{d\varepsilon_{\mathbf{k}}}=\cos^2\theta .$$

Hence since $N_s^{-1}=\rho_0\int d\varepsilon_{\mathbf{k}}$, then (A1) becomes

$$S=\rho_0\int dE_{\mathbf{k}}\frac{\sin^2(2\theta_{\mathbf{k}})}{E_{\mathbf{k}}}\tanh\left(\frac{\beta E_{\mathbf{k}}}{2}\right). \tag{A2}$$

Hence, using (4.2) we have (abbreviating $\langle b\rangle$ to b)

$$S=\rho_0 b^2V^2\int_{\varepsilon_-^-}^{\varepsilon_+^-}\frac{dE}{E}\frac{1}{(\varepsilon_d-E)^2+b^2V^2}\tanh\left(\frac{\beta E}{2}\right), \tag{A3}$$

where energies are with respect to μ as energy zero, and the cutoffs for the lower quasiparticle (hole) band are specifically inserted.

In order to evaluate S to logarithmic accuracy we may approximate (A3) by

$$S=\rho_0 b^2V^2\left[-\int_{\varepsilon_-^-}^{c}+\int_{c}^{\varepsilon_+^-}\right]\frac{dE}{E}\frac{1}{(\varepsilon_d-E)^2+b^2V^2}, \tag{A4}$$

where $c=T/1.14$. The coefficient c is chosen so that were $[(\varepsilon_d-E)^2+b^2V^2]$ energy independent, (A4) reproduces (A3) correctly, thus building in logarithmic accuracy.

Now (A4) may be evaluated, obtaining to logarithmic accuracy

$$S=\frac{\rho_0 b^2V^2}{(\varepsilon_d-\mu)^2+b^2V^2}\left[\ln\left(\frac{\varepsilon_-^- -\mu}{[(\varepsilon_-^- -\varepsilon_d)^2+b^2V^2]^{1/2}}\right)+\ln\left(\frac{\varepsilon_+^- -\mu}{[(\varepsilon_+^- -\varepsilon_d)^2+b^2V^2]^{1/2}}\right)-2\ln\left(\frac{c}{[(c-\varepsilon_d)^2+b^2V^2]^{1/2}}\right)\right]. \tag{A5}$$

Now $\varepsilon_d-\mu\simeq bV(bV/D)$, suggesting that for sufficiently small b we may assume the b^2V^2 terms are the largest in the square roots in (A5). This approximation gives us a simple result for S

$$S\simeq 2\rho_0\ln\left(\frac{1.14\omega_c}{T}\right), \tag{A6}$$

where $\omega_c=[(\varepsilon_-^- -\mu)]^{1/2}$. Substituting (A6) into (4.10) yields (4.11). Next we wish to evaluate to logarithmic accuracy the sum

$$S'=(V^2/4N_s)\sum_{\mathbf{k}}\frac{\sin^2(2\theta_{\mathbf{k}})}{(E_{\mathbf{k}}^2+\Delta^2)^{1/2}}, \tag{A7}$$

where $\Delta=\Delta_{\mathbf{k}_F}$. Following the previous derivation, S' may be written

$$S'=\rho_0 b^2V^2\int_{\varepsilon_-^-}^{\varepsilon_+^-}\frac{dE}{[(\varepsilon_d-E)^2+b^2V^2]^{1/2}(E^2+\Delta^2)}. \tag{A8}$$

By a similar ansatz to that in (A4), (A8) is approximated by

$$S'=\rho_0 b^2V^2\left[-\int_{\varepsilon_-^-}^{c'}+\int_{c'}^{\varepsilon_+^-}\right]\frac{dE}{[(\varepsilon_d-E)^2+b^2V^2]E}. \tag{A9}$$

where now $c'=\Delta/2$. Hence from (A6)

$$S'=2\rho_0\ln\left(\frac{2\omega_c}{\Delta}\right). \tag{A10}$$

APPENDIX B

In this appendix we consider the extension of the Langrangian density of Eq. (5.1b) to bosons of higher symmetry, i.e.,

$$Z=\int_{-\pi/\beta}^{\pi/\beta}\prod_i\left(\frac{\beta d\lambda_i}{2\pi}\right)\int DbDb^\dagger Da_{mn}Da_{mn}^\dagger Dd_nDd_n^\dagger Dc_{\mathbf{k}m}Dc_{\mathbf{k}m}^\dagger\left[\exp\left(-\int_0^\beta d\tau L(\tau)\right)\right], \tag{B1}$$

where

$$\begin{aligned}L(\tau)=&\sum_i b^\dagger(\mathbf{r}_i)\left(\frac{d}{d\tau}+E_0\right)b(\mathbf{r}_i)+\sum_{i,m,n}a_{mn}^\dagger(\mathbf{r}_1)\left(\frac{d}{d\tau}+E_2\right)a_{nm}(\mathbf{r}_i)\\&+\sum_{im}d_m^\dagger(\mathbf{r}_i)\left(\frac{d}{d\tau}+E_1\right)d_m(\mathbf{r}_i)+\sum_{\mathbf{k}m}c_{\mathbf{k}m}^\dagger\left(\frac{d}{d\tau}+\varepsilon_{\mathbf{k}}\right)c_{\mathbf{k}m}\\&+\sum_{\mathbf{k}mi}[V_{\mathbf{k}}b(\mathbf{r}_i)d_m^\dagger c_{\mathbf{k}m}e^{i\mathbf{k}\cdot\mathbf{r}_i}+\text{H.c.}]+\sum_{\mathbf{k}mni}[V_{\mathbf{k}}a_{mn}^\dagger(\mathbf{r}_i)d_mc_{\mathbf{k}m}e^{i\mathbf{k}\cdot\mathbf{r}_i}\operatorname{sgn}\sigma+\text{H.c.}]\\&+i\sum_{imn}\lambda_i[d_m^\dagger(\mathbf{r}_i)d_m(\mathbf{r}_i)+b^\dagger(\mathbf{r}_i)b(\mathbf{r}_i)+a_{mn}^\dagger(\mathbf{r}_i)a_{nm}(\mathbf{r}_i)-1].\end{aligned} \tag{B2}$$

This is a $SU(p)\times U(1)$ form of the Lagrangian. Here N is the number of independent components of the antisymmetric tensor $a_{mn}(\mathbf{r}_i)$. If m and n run from 1 to p, then $N=p(p-1)/2$. U(1) accounts for the phase and amplitude of $a_{mn}(\mathbf{r}_i)$. The index Rm should not be confused with Eq. (2.11). What are the physical possibilities for such a generalization? Suppose the localized d_m manifold has m degenerate states. (For the CuO plane without crystal-field splitting m would equal 5 per spin) and suppose the d-k hybridization conserved angular momentum, then Eq. (B2) would be relevant. When the representation of an occupied point group of the manifold m is greater than one, Eq. (B2) will split into smaller invariants. For Cu-O the partially occupied manifold is believed to be 1 (with, of course, two spins), in which limit Eq. (B2) reduces to Eq. (5.1b). Equation (B2) after integration over the b, d, and c fields gives the following LG free-energy density:

$$\begin{aligned}\beta f(\mathbf{x})=&\sum_{mn}\{\tfrac{1}{2}r(0)[a_{mn}^1(\mathbf{x})a_{nm}^1(\mathbf{x})+a_{mn}^2(\mathbf{x})a_{nm}^2(\mathbf{x})]+[\nabla_\parallel a_{mn}^1(\mathbf{x})\cdot\nabla_\parallel a_{nm}^1(\mathbf{x})+\nabla_\parallel a_{mn}^2(\mathbf{x})\cdot\nabla_\parallel a_{nm}^2(\mathbf{x})]\}\\&\times\gamma^2\left(\frac{\partial}{\partial z}a_{mn}^1(\mathbf{x})\frac{\partial}{\partial z}a_{nm}^1(\mathbf{x})\right)+\gamma^2\left(\frac{\partial}{\partial z}a_{mn}^2(\mathbf{x})\frac{\partial}{\partial z}a_{nm}^2(\mathbf{x})\right)\\&+\sum_{m_1m_2n_1n_2}(v(0)\{[a_{m_1n_1}^1(\mathbf{x})\cdot a_{n_1m_1}^1(\mathbf{x})]^2+[a_{m_2n_2}^2(\mathbf{x})\cdot a_{n_2m_2}^2(\mathbf{x})]^2\}\\&+u(0)[a_{m_1n_1}^1(\mathbf{x})a_{n_1m_1}^1(\mathbf{x})a_{m_2n_2}^1(\mathbf{x})a_{n_2m_2}^1(\mathbf{x})+a_{m_1n_1}^2(\mathbf{x})a_{n_1m_1}^1(\mathbf{x})a_{m_2n_2}^2(\mathbf{x})a_{n_2m_2}^2(\mathbf{x})\\&+2a_{m_1n_1}^1(\mathbf{x})a_{n_1m_1}^1(\mathbf{x})a_{m_2n_2}^2(\mathbf{x})a_{n_2m_2}^2(\mathbf{x})])\,,\end{aligned} \tag{B3}$$

where the superscripts 1 and 2 refer to the real and imaginary components of a_{mn}, namely $a_{mn}=a_{mn}^1+ia_{mn}^2$. We have evaluated the flow equation for $r(l)$, $u(l)$, and $v(l)$ for arbitrary N of Eq. (B3) to linear order in ε. After a lengthy calculation which is somewhat similar to Refs. 47 and 48, we get

$$\frac{dr(l)}{dl}=2r(l)+K_4\left(\frac{R_uu(l)+R_vv(l)}{1+r(l)}\right), \tag{B4}$$

$$\frac{du(l)}{dl}=\varepsilon u(l)-K_4\left(\frac{R_{uu}u^2(l)+R_{uv}u(l)v(l)}{[1+r(l)]^2}\right), \tag{B5}$$

and

$$\frac{dv(l)}{dl}=\varepsilon v(l)-K_4\left(\frac{S_{vv}v^2(l)+S_{uv}u(l)v(l)+S_{uu}u^2(l)}{[1+r(l)]^2}\right), \tag{B6}$$

where $R_u=4p-2$, $R_v=2p^2-2p+8$, $R_{uu}=5p-4$, $S_{uv}=48$, $S_{vv}=4p^2-4p+32$, $S_{uv}=12p-8$, $S_{uu}=7$ [recall that $N=p(p-1)/2$]. Equation (B3) has four fixed points:

$$u^*(0)=0,\quad v^*(0)=0\,, \tag{B7}$$

$$u^*(0)=0,\quad v^*(0)=\frac{\varepsilon}{K_4S_{vv}}\,, \tag{B8}$$

$$v_\pm^*(0)=\varepsilon\frac{-b+(b^2-4ac)^{1/2}}{2}\,,\quad u^{+*}(0)=\frac{\varepsilon-K_4R_{uv}v_\pm^*(0)}{K_4R_{uu}}\,, \tag{B9}$$

and

$$v^{*}_{\pm}(0)=\varepsilon\frac{-b-(b^2-4ac)^{1/2}}{2}, \qquad u^{+*}(0)=\frac{\varepsilon-K_4R_{uv}v^{*}_{\pm}(0)}{K_4R_{uu}}. \tag{B10}$$

The corresponding fixed point for r is given by

$$r^{*}=K_4[R_u u^{*}(0)+R_v v^{*}(0)]. \tag{B11}$$

For Eqs. (B7)-(B10)

$$a=K_4\left[S_{vv}-\frac{S_{uv}R_{uv}}{R_{uu}}+\frac{S_{uu}R_{uv}^2}{R_{uu}^2}\right], \tag{B12}$$

$$b=\frac{S_{uv}}{R_{uu}}-\frac{2S_{uu}R_{uv}}{R_{uu}}-1, \tag{B13}$$

and

$$c=\frac{S_{uu}}{K_4R_{uu}^2}. \tag{B14}$$

The corresponding exponent ν (which relates to the specific-heat exponent $\alpha=2-d\nu$) for the four fixed points is given by

$$\nu=\frac{1}{2}\left[1+\frac{K_4}{2}[R_u u^{*}(0)+R_v v^{*}(0)]\right], \tag{B15}$$

and the two crossover exponents ϕ_+ and ϕ_- (which determine the stability of the fixed points) are

$$\phi_{\pm}=\frac{\varepsilon}{2}\{-(a_{11}+a_{22})\pm[(a_{11}+a_{22})^2-4(a_{11}+a_{22}-a_{12}a_{21})]^{1/2}\}, \tag{B16}$$

$$a_{11}=1-\frac{K_4}{\varepsilon}[2R_{uu}u^{*}(0)+R_{uv}v^{*}(0)], \tag{B17}$$

$$a_{12}=-\frac{K_4}{\varepsilon}R_{uv}u^{*}(0), \tag{B18}$$

$$a_{21}=-\frac{K_4}{\varepsilon}[2S_{uu}u^{*}(0)+S_{uv}v^{*}(0)], \tag{B19}$$

and

$$a_{22}=1-\frac{K_4}{\varepsilon}[S_{uv}u^{*}(0)+S_{vv}v^{*}(0)]. \tag{B20}$$

We, of course, recognize that these results are premature for any experimental implication; this might not be so forever. In particular, superconductivity in the heavy-fermion systems, with large f-shell degeneracy, might be an appropriate system; future high-T_c materials might also become relevant.

[1] L. F. Mattheiss, Phys. Rev. Lett. **58**, 1028 (1987); L. F. Mattheiss and D. R. Hamann (unpublished).

[2] J. Yu and A. J. Freeman, Phys. Rev. Lett. **58**, 1035 (1987).

[3] W. E. Pickett, H. Krakauer, D. A. Papaconstantopoulos, and L. L. Bogen, Phys. Rev. B **35**, 7252 (1987).

[4] D. Vaknin, S. K. Sinha, D. E. Moncton, D. C. Johnston, H. E. King, J. M. Newsam, and C. R. Safinya, Phys. Rev. Lett. **58**, 2802 (1987).

[5] B. Reihl, T. Riesterer, T. G. Bednorz, and K. A. Müller, Phys. Rev. B **35**, 8804 (1987).

[6] L. Hoffman, A. A. Manuel, M. Peter, E. Walker, and M. A. Damento, in *Proceedings of the Conference on High Temperature Superconductors, Materials and Mechanics of Superconductivity, Interlaken 1988,* edited by J. Müller and J. L Olsen [Physica C **153–155**, 129 (1988)].

[7] S. Tajima, S. Uchida, S. Kanke, K. Kitazawa, K. Fueki, and S. Tanaka, in *Proceedings of the 18th International Conference on Low Temperature Physics, Kyoto, 1987* [Jpn. J. Appl. Phys. **26**, Suppl. 26-3, 1007 (1987)]; Z. Schlesinger, R. T. Collins, D. L. Kaiser, and F. Holtzberg, Phys. Rev. Lett. **59**, 1958 (1982).

[8] A. Junod, A. Bezinge, D. Caltani, J. Cors, M. Decroux, O. Fischer, P. Genoud, L. Hoffman, J.-L. Jorda, J. Muller, and E. Walker, in *Proceedings of the 18th International Conference on Low Temperature Physics, Kyoto, 1987* [Jpn. J. Appl. Phys. **26**, Suppl 26-3, 1119 (1987)]; S. von Molnar, A. Torresen, D. Kaiser, F. Holtzberg, and T. Penney, Phys. Rev. B **37**, 3762 (1988).

[9] R. L. Greene, H. Maletta, T.-S. Plaskett, J. G. Bednorz, and K. A. Müller, Solid State Commun. **63**, 379 (1987); H. Takagi, S. Uchida, M. Sato, K. Kishio, K. Kitazawa, K. Fueki, and S. Tanaka, in *Proceedings of the 18th International Conference on Low Temperature Physics, Kyoto, 1987* [Jpn. J. Appl. Phys. **26**, Suppl 26-3, 1015 (1987)].

[10] N. Nucker, J. Fink, B. Renker, D. E. Wart, P. J. W. Weijs, and J. C. Fuggle, in *Proceedings of the 18th International Conference on Low Temperature Physics, Kyoto, 1987* [Jpn. J. Appl. Phys. **26**, Suppl. 26-3, 1015 (1987)].

[11] W. R. McGrath, H.-K. Olsson, T. Claeson, S. Ercksson, and L.-G. Johnasson, Europhys. Lett. **4**, 357 (1987).

[12] D. R. Harshman, G. Aeppli, E. J. Ansaldo, B. Batlogg, J. H. Brewer, J. F. Carolan, R. J. Cava, M. Celio, A. C. D. Chaklader, N. N. Hardy, S. R. Kreitzman, G. M. Luke, D. R. Noakes, and M. Senba, Phys. Rev. B **36**, 2386 (1987).

[13] I. Furo, A. Janossy, L. Mihaly, P. Banky, I. Pocsik, and I. Bakonyi (unpublished).

[14] J. R.Kirtley, C. C. Tsuei, S. I. Park, C. C. Chi, J. Rozen, M. W. Shafer, W. J. Gallagher, R. L. Sandstrom, T. R. Dinger, and D.-A. Charue, in *Proceedings of the 18th International Conference on Low Temperature Physics, Kyoto, 1987* [Jpn. J. Appl. Phys. **26**, Suppl. 26-3, 997 (1987)]; J. R. Kirtley (private communication).

[15] M. Strongin (private communication).

[16] B. Batlogg, R. J. Cava, A. Jayaraman, R. B. van Dover, G. A. Kourouklis, S. Sunshine, D. W. Murphy, L. W. Rupp, H. S. Chen, A. White, K. T. Short, A. M. Mujsce, and E. A. Rietman, Phys. Rev. Lett. **58**, 2333 (1987); B. Batlogg, G. Kourouklis, W. Weber, R. J. Cava, A. Jayaraman, A. E. White, K. T. Short, L. W. Rupp, and E. A. Rietman, *ibid.* **59**, 912 (1987).

[17] T. R. Worthington, W. J. Gallagher, and T. R. Dinger, Phys. Rev. Lett. **59**, 1160 (1987).

[18] Z. Z. Wang, J. Clayhold, N. P. Ong, J. M. Tarascon, L. M. Greene, W. R. McKinnon, and G. W. Mull, Phys. Rev. B **36**, 7222 (1987).

[19] N. P. Ong, Z. Z. Wang, J. Clayhold, J. M. Tarascon, L. M.

Greene, and W. R. McKinnon, Phys. Rev. B **35**, 8807 (1987).
[20]M. W. Shafer, T. Penney, and B. L. Olson, Phys. Rev. B **36**, 4047 (1987).
[21]K. Miyake, T. Matsuura, and Y. Nagaoka (unpublished).
[22]Z.-X. Shen, J. W. Allen, J. J. Yeh, J.-S. Kang, W. Ellis, W. E. Spicer, I. Lindau, M. B. Maple, Y. D. Dalichaouch, M. S. Torikachvili, J. Z. Sun, and T. H. Geballe, Phys. Rev. B **36**, 8414 (1987); J. A. Yarmoff, D. R. Clarke, W. Drube, U. O. Karlsson, A. Taleb-Ibrahimi, and F. J. Himpsel, *ibid.* **36**, 3967 (1987); T. Miyahard, S. Mosoya, M. Sato, *Proceeding of the 18th International Conference on Low Temperature Physics, Kyoto, 1987* [Jpn. J. Appl. Phys. **26**, Suppl. 26-3, 1013 (1987)]; P. Thiry, G. Rossi, Y. Petroff, A. Revcolevschi, and J. Jegoudez (unpublished).
[23]D. M. Newns, Adv. Phys. **36**, 799 (1987).
[24]P. W. Anderson, Science **235**, 1196 (1987); P. W. Anderson, G. Baskaran, G. Zou, and T. Hsu, Phys. Rev. Lett. **58**, 2790 (1987); G. Baskaran, Z. Zou, and P. W. Anderson (unpublished).
[25]A. Ruckenstein, P. Hirschfeld, and J. Appel. Phys. Rev. B **36**, 857 (1987); M. Inui, S. Doniach, P.-J. Hirschfeld, and A. E. Ruckenstein, *ibid.* **37**, 2320 (1988).
[26]G. Kotliar (unpublished); M. Nauenberg, Phys. Rev. B **36**, 7207 (1987); P.-A. Lee, G. Kotliar, and N. Read (unpublished).
[27]H. Fukuyama and K. Yosida, Jpn, J. Appl. Phys. **26**, 160 (1987).
[28]D. M. Newns, Phys. Rev. B **36**, 5595 (1987).
[29]D. M. Newns, Phys. Rev. B **36**, 2429 (1987).
[30]M. Imada, in *Proceedings of the 18th International Conference on Low Temperature Physics, Kyoto, 1987* [Jpn. J. Appl. Phys. **26**, Suppl. 26-3, 985 (1987)]; M. Imada (unpublished).
[31]J. E. Hirsch, Phys. Rev Lett. **59**, 228 (1987); J. Hirsch and M. Q. Liu (unpublished).
[32]V. J. Emery, Phys. Rev. Lett. **58**, 2794 (1987).
[33]S. Sachdev and R. Shankar, Phys. Rev. B **38**, 826 (1988).
[34]C. J. Pethick and David Pines (unpublished).
[35]K. Machida, in *Proceedings of the 18th International Conference on Low Temperature Physics, Kyoto, 1987* [Jpn. J. Appl. Phys. **26**, Suppl. 26-3, 1155 (1987)]; M. Kato, Y. Suzumura, Y. Okabe, and K. Machida (unpublished).
[36]S. E. Barnes, J. Phys. F **6**, 1375 (1975); **7**, 2637 (1977).
[37]Y. Isawa, S. Maekewa, and H. Ebisawa (unpublished).
[38]N. Read, Ph. D. Thesis, University of London, 1985 (unpublished); N. Read and D. M. Newns, J. Phys. C **16**, 3273 (1983); **16**, L1055 (1983); N. Read, **18**, 2651 (1985); D. M. Newns, N. Read, and A. C. Hewson, in *Moment Formation in Solids,* edited by W. L. Buyers (Plenum, New York, 1984); N. Read and D. M. Newns, Solid State Commun. **52**, 993 (1984).
[39]P. Coleman, Phys. Rev. B **28**, 5255 (1983); **29**, 3035 (1984); **35**, 5072 (1984).
[40]A. Auerbach and K. Levin, Phys. Rev. Lett. **57**, 877 (1986).
[41]A. J. Millis and P. A. Lee, Phys. Rev. B **35**, 3394 (1987).
[42]G. t'Hooft, Nucl. Phys. **B72**, 461 (1974).
[43]M. Lavagna, A. J. Millis, and P. A. Lee, Phys. Rev. Lett. **58**, 266 (1987).
[44]A. Houghton, N. Read and H. Won, Phys. Rev. B **37**, 3782 (1988).
[45]P. B. Allen and B. Mitrovic, in *Solid State Physics,* edited by H. Ehrenreich, F. Seitz, and D. Turnbull (Academic, New York, 1982), Vol. 37, p. 1.
[46]M. Rasolt, M. J. Stephen, M. E. Fisher, and P. B. Weichman, Phys. Rev. Lett. **53**, 798 (1984); Phys. Rev. B **33**, 4632 (1986).
[47]J. Rudnick and D. Nelson, Phys. Rev. B **16**, 2032 (1977).
[48]J. F. Micoll and T. S. Chang, Phys. Rev. A **17**, 2083 (1978).
[49]D. M. Newns, P. Pattnaik, M. Rasolt, and D. A. Papaconstantopoulos, this issue, Phys. Rev. B **38**, 7033 (1988).
[50]K. Miyake and Y. Nagaoka, in *Superconducting Materials* [Jpn. J. Appl. Phys. Ser. 1, 220 (1988)].
[51]M. Schluter and M. S. Hybertson (unpublished).
[52]E. Stechel and D. R. Jennison, Phys. Rev. B **38**, 4632 (1988).
[53]A. K. McMahan, R. M. Martin, and S. Satpathy, this issue, Phys. Rev. B **38**, 6650 (1988).
[54]A. Houghton and A. Sudbo, this issue, Phys. Rev. B **38**, 7037 (1988).
[55]J. R. Schrieffer, X. G. Wen, and S. C. Zhang, Phys. Rev. Lett. **60**, 944 (1988).
[56]J. B. Torrance (unpublished).